IEEE Access
Multidisciplinary ⋮ Rapid Review ⋮ Open Access Journal

Received 19 June 2023, accepted 24 July 2023, date of publication 28 July 2023, date of current version 4 August 2023.

Digital Object Identifier 10.1109/ACCESS.2023.3299859

TOPICAL REVIEW

Application of Triboelectric Nanogenerators on Manipulators

ZHONGYANG XU, JIABIN ZHANG, JUNHAN HUANG, ZHONGXIAN WANG, AND YONG SHI

School of Mechanical Engineering, Heilongjiang University, Harbin 150001, China

Corresponding author: Shi Yong (sy_hit@163.com)

ABSTRACT The exacerbation of the energy crisis has led to the development of various self-powered sensors, resulting in rapid advancements in the energy field. The sensor based on the triboelectric nanogenerator (TENG) is particularly effective in collecting mechanical energy from low-frequency and irregular movement. It can convert external mechanical forces directly into electrical signals, making it a self-powered (or self-driven) sensor. High-performance TENGs are widely used in flexible sensing, implantable power supplies, healthcare, and biomedical applications. This paper introduces TENG power generation methods, advantages, and disadvantages of TENG, summarizes the related research of TENG simulation, material selection, sensor fabrication, etc., and reviews applied research of TENG in manipulators. Finally, the current challenges and problems facing TENG-based sensors are discussed, and the future development of TENG technology is explored.

INDEX TERMS Self-powered, TENG, triboelectric material, flexible sensing, manipulators.

I. INTRODUCTION

The current energy crisis has led to extensive research on self-powered sensors that use various technologies such as triboelectricity, piezoelectricity, capacitance, and batteries [1], [2], [3]. Among these, the triboelectric nanogenerator (TENG) is a device that converts mechanical energy into electrical energy by utilizing the triboelectric effect and electrostatic induction [4]. The TENG typically consists of a metal electrode coated or plated on one side of two different polymers to form an electrical output electrode, while the other side of the polymer serves as the triboelectric surface [5]. The TENG can be used to collect various forms of mechanical energy, such as human motion [6], mechanical vibration [7], wind energy [8], wave energy [9], rotation [10], sound waves [11], and raindrops [12]. However, the TENG has applications beyond power generation, such as serving as a self-powered sensor to detect physical parameters like velocity [13], [14], [15], metal ions [16], humidity [17], temperature [18], etc.

Considering that there is a certain relationship between the mechanical excitation of TENG and the electrical signal generated, the mechanical signal can be measured by analyzing the electrical signal [19], [20], [21]. Moreover, TENGs are frequently composed of elastic materials, which provides them with unique advantages in adapting to diverse environments compared to other sensors [22]. As a result, TENGs have attracted considerable attention in areas such as tactile sensing for the human body and perception and actuation for biomimetic robotic hands [23].

In recent years, with the increasing demand for intelligence and wearable technologies, triboelectric nanogenerators (TENGs) have gradually become a research hotspot. TENG, as a self-powered sensor, possesses unique energy conversion mechanisms and material flexibility, enabling efficient energy harvesting and sensitive sensing in applications such as manipulators, while also demonstrating a wide range of potential uses. By further optimizing the design and structure of TENGs, researchers are striving to enhance their output performance and improve their mechanical properties to achieve more reliable self-powered sensing capabilities [24].

Furthermore, the emergence of soft robots has sparked widespread enthusiasm for flexible and soft sensors and actuators [25], [26]. Due to their low modulus and high flexibility, flexible and soft sensors and actuators can be easily integrated into soft robots, allowing for safer interaction with humans or the environment and relatively unrestricted

The associate editor coordinating the review of this manuscript and approving it for publication was Roberto C. Ambrosio.

movement [27], [28]. By combining advanced materials science and nanotechnology, more sensitive, reliable, and customizable TENG sensors can be developed to meet precise sensing and responsive requirements. The application of TENG-based systems theoretically overcomes the current challenges in mapping and integration faced by traditional mechanical systems, and addresses the shortcomings of robots in terms of workspace, task objects, and human-machine collaboration, to meet the increasingly complex task demands.

This paper provides a comprehensive review of the fabrication, measurement, and application of flexible-triboelectric-nanogenerator(TENG)-based sensors in robotics. Firstly, the four basic working modes of TENGs are summarized, and their respective advantages and limitations are analyzed in detail. Subsequently, the current state-of-the-art research and technological advancements in TENG fabrication, measurement, performance evaluation, and simulation are discussed. Finally, the paper highlights examples of TENG-based sensors applied in robotic hands and provides insights into the prospects of TENGs in this field.

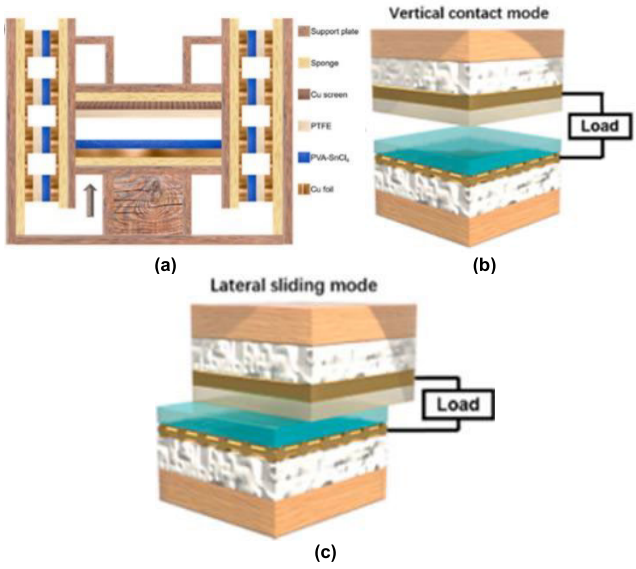

FIGURE 1. (a) Schematic illustration of the hybrid motion mode TENG; (b) vertical contact mode; (c) lateral sliding mode [40].

II. APPLICATIONS OF TRIBOELECTRIC NANOGENERATORS

There are four working modes of TENGs: vertical contact-separation mode, lateral sliding mode, single-electrode mode, and freestanding triboelectric-layer mode [29].

Table 1 summarizes the recent research on TENGs in robotic hands, including the working modes used in each study.

Table 1 indicates that the Vertical Contact-Separation and Single-Electrode Modes are widely used in robotic hands due to their simple structure and high instantaneous output energy, while the freestanding triboelectric-layer mode and lateral sliding mode have their advantages in specific applications. However, it is important to note that each TENG theoretical model has its strengths and weaknesses, which are summarized in Table 2.

The optimal TENG model can be designed by combining various theoretical models according to practical application scenarios. For instance, Xu et al. [40] combined the vertical contact-separation mode and the lateral sliding mode to create a hybrid-mode TENG (Fig. 1). The peak open-circuit voltage of the hybrid-mode TENG reached 1169 V, and the unidirectional short-circuit current of the hybrid TENG reached 187μA. Based on this design, a self-powered human motion sensor was developed to detect finger bending, gait, and body joint angles. This sensor accurately identified motion signals from different body parts.

III. TENG-RELATED RESEARCH ON MANIPULATORS

A. THE MODELING AND SIMULATION OF TENG

The finite element simulation provides the visualization of how the charges in the circuit are driven during the operation of TENG, allowing a deeper understanding of the relationship between mechanical energy and electrical energy conversion and providing a theoretical foundation for the development of high-efficiency TENGs [41]. For example, Mainra et al. [42] used modeling and simulation to investigate the effects of varying the thickness of the triboelectric layer on the output voltage of TENGs with three different materials for triboelectric layers. The results showed that the output voltage initially increased linearly with the increase in triboelectric layer thickness but then started to decrease. Similarly, Mathew and Vivekanandan [43] designed a twodimensional model of a single-electrode mode TENG (SETENG) for harvesting wrist pulses and optimized the materials, thickness, and surface morphology of SE-TENG to achieve maximum output voltage. Finite element simulations generally focus on three aspects:

1) DESIGN OPTIMIZATION

Simulation-based optimization enhances the performance and power generation efficiency of TENGs by optimizing their structure, shape, size, and materials. For instance, Yin et al. [44] proposed a parallel unit PC-TENG (Fig. 2) that generates significantly more electrical output than the traditional Z-TENG. The authors used a simulation model to optimize three critical components of PC-TENG, namely the electrodes, triboelectric layer, and substrate, to achieve higher output power with the same mechanical input. They also conducted numerical simulations of PC-TENG and ZTENG using Comsol software to validate their design and performance. Based on these simulations, the authors concluded that the optimized design of PC-TENG has superior mechanical energy conversion efficiency and stability.

Adly et al. [45] developed a Triboelectric inertial motion sensor and investigated its electromechanical coupling performance both theoretically and experimentally. They vali-

TABLE 1. Applications of various working modes of TENG on mechanical hands.

Time	Author	Research topic	Work mode	Advantages
2018	Inkyum Kim[30]	All-in-one cellulose based triboelectric nanogenerator for electronic paper using simple filtration process	Vertical Contact-Separati-on Mode	The designed all-fiber-based TENG shows the superior foldable characteristic and stable sheet resistance in hard mechanical stress of folding
2019	Xie[31]	Spiral Steel Wire Based Fiber-Shaped Stretchable and Tailorable Triboelectric Nanogenerator for Wearable Power Source and Active Gesture Sensor	Single-Electrode Mode	The system exhibits flexibility, good compatibility, and high accuracy in electrical signal recognition.
2019	Zhang[32]	Self-Powered Triboelectric-Mechanoluminescent Electronic Skin for Detecting and Differentiating Multiple Mechanical Stimuli	Vertical Contact-Separati-on Mode	When used as a contact-separation mode TENG, it exhibits a maximum sensitivity of 2 V/N.
2019	Wang[33]	Large-Area Integrated T triboelectric Sensor Array for Wireless Static and Dynamic Pressure Detection and Mapping	Vertical Contact-Separati-on Mode	The device is flexible and durable, capable of sensing both flexible and durable, while also capable of sensing both flexible and capable of sensing static and dynamic pressure from the external environment.
2019	Zheng[34]	Dual-Stimulus Smart Actuator and Robot Hand Based on a Vapor-Responsive PDMS Film and Triboelectric Nanogenerator	Freestanding Triboelectric-Layer Mode	The device provides a safe, high static voltage that poses no risk to researchers and can serve as a self-powered system using TENG without external power sources.
2019	Smitha Ankanahalli Shankaregowda [35]	Single-electrode triboelectric nanogenerator based on economic graphite coated paper for harvesting waste environmental energy	Single-Electrode Mode	The device can efficiently harvest energy from hand clapping and generate a maximum open-circuit voltage of up to 320 V for GCP-TENG.
2019	Lai[36]	Single-Thread-Based Wearable and Highly Stretchable Triboelectric Nanogenerators and Their Applications in Cloth-Based Self-Powered Human-Interactive and Biomedical Sensing	Single-Electrode Mode	The devices are simple yet reliable, useful, and efficient, and the processes are cost-effective and suitable for industrial manufacture.
2022	Zhang[37]	Nondestructive Dimension Sorting by Soft Robotic Grippers Integrated with Triboelectric Sensor	Freestanding Triboelectric-Layer Mode	The gripper is capable of nondestructive grasping, size measurement, and precise sorting. The measurement error rate is only 2.22%.
2022	Hyosik Park[38]	Plasticized PVC-Gel Single Layer-Based Stretchable Triboelectric Nanogenerator for Harvesting Mechanical Energy and Tactile Sensing	Vertical Contact-Separati-on Mode	The method of introducing plasticized PVC-gel can generate high output power, and dozens of LEDs can be lit with a simple touch.

dated the model by designing a low-cost device (Figure 3) and conducted parameter studies to differentiate the influence of various device parameters. A hybrid particle swarm optimization (PSO) and direct search technique were employed to improve some device parameters. Experimental tests were carried out over an input acceleration range from 0.4 g to 1.2 g, and target functions for output voltage density, i.e., peak output voltage per unit volume, were formulated for different excitation frequencies and various design parameters. A comparison between the theoretical model and experimental measurement results demonstrated the practicality and effectiveness of the optimization techniques used, emphasizing their potential applications in other triboelectric applications.

Chen et al. [46] systematically investigated the influence of reference electrodes on the performance of single-electrode triboelectric nanogenerators (SETENGs) through theoretical simulations and experimental validations. The paper presented an analysis and optimal design of the reference electrodes for both the Contact-Separation Mode SETENG, called P-CS-SETENG (with the main electrode as the triboelectric layer), and the Sliding Mode SETENG, as well as the study of SETENG with an additional dielectric layer structure attached to the main electrode. The authors found that factors such as the position, as shown in Figure 4, shape, and distance from the main electrode to the reference electrode all affect the output performance of SETENGs. They proposed targeted strategies, including positioning the reference electrode offset from the main electrode, maximizing the area of the reference electrode while not exceeding the main electrode's area, and keeping the distance between the reference electrode and the main electrode as far as possible without exceeding the maximum separation distance, among others. Experimental validations demonstrated that the results were in good agreement with the theoretical simulations, confirming the reliability of the theoretical modeling. These findings provide important theoretical guidance and an experimental foundation for the design and optimization of SETENGs.

Roopa et al. [47] argue that the complexity of the experimental process, the demand for multiple manufacturing techniques, extensive characterization, cost, and time can be significantly reduced through simulation when using new materials or multiple material systems in practical experiments. They employed COMSOL to simulate a simple, inexpensive, and scalable method for constructing a

TABLE 2. Types of TENGs and their pros and cons [39].

TENG Type	Advantages	Limitations
Vertical Contact-Separation Mode	Structurally simple, easy to fabricate, with instantaneous high output, suitable for multilayer integration	The friction materials are prone to wear
Lateral Sliding Mode	The energy conversion efficiency is high, with diverse forms and easy integration and packaging, making it widely applicable	The device occupies a large area
Single-Electrode Mode	Lightweight, wear-resistant, and highly flexible in the operational state, making it ideal for self-driven sensors application	The low efficiency of energy collection
Freestanding Triboelectric-Layer Mode	Diverse forms, improved durability, and higher current in comparison to single-electrode mode	Unstable energy signals

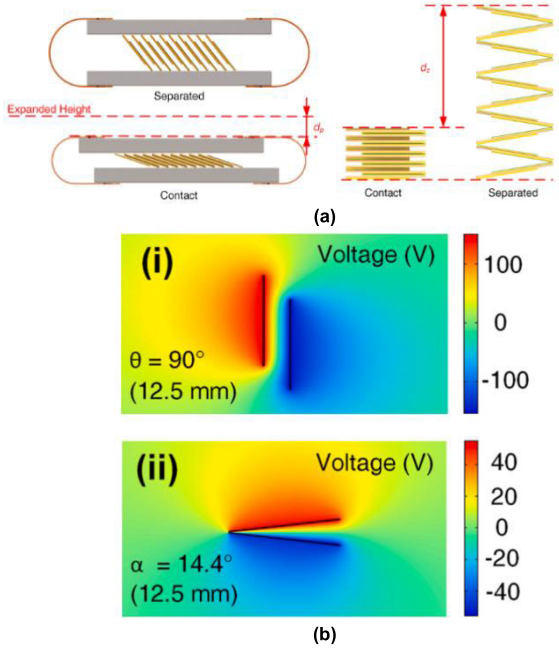

FIGURE 2. (a) Contact and separated states of PC-TENG and Z-TENG (b) Simulated open-circuit voltage of a triboelectric cell [44].

triboelectric nanogenerator with an extremely high electrical yield, as shown in Figure 5. The nanogenerator consisted of polydimethylsiloxane (PDMS), gold, and polymethyl methacrylate (PMMA) with gold nanoparticles. Aluminum and copper were used as alternatives to gold in the experiments. Through simulations, the PDMS polymer thickness was optimized to 10 mm, resulting in a maximum voltage of the order of 103 volts. The vertical contact-mode generator with gold-coated electrodes generated an expected power of 15 mW.

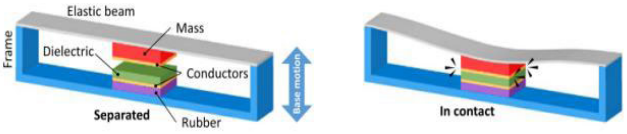

FIGURE 3. Schematic illustration of the proposed device [45].

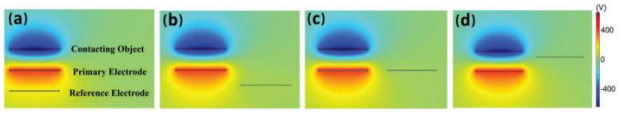

FIGURE 4. The effect of the reference electrode's location on the output performance of the P-CS-SETENG. a-d) Images showing the reference electrode placed at (a) below, (b) below right, (c) right, and (d) upper right of the primary electrode [46].

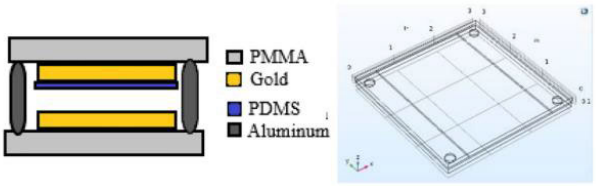

FIGURE 5. (a) Proposed TENG module; (b) Structure simulated using the tool [47].

2) CHARACTERIZATION OF PERFORMANCE

Simulation can be used to evaluate the performance indicators of TENG, such as output voltage, output power, linearity, etc. Cheng et al. [48] simulated and studied the effect of temperature difference on the performance of TENGs by combining the electron-cloud-potential-well model for tribo-electrification and the thermionic-emissi-on model. They also designed and fabricated a temperature-difference TENG to improve the power output performance in high-temperature environments.

Bhatta et al. [49] introduced a new S-PVDF composite nanofiber membrane and incorporated experimental data on surface charge density into a COMSOL model. By simulating the surface potential of the TENG at various gap distances (mm) between TENG layers (Fig. 7), the authors established a relationship between the potential and the gap distance, where the potential increased as the gap distance increased. After optimizing the device volume, a gap of 2mm was selected between the two layers. The experimental results confirmed the accuracy and reliability of the simulation calculations.

3) VISUALIZATION

The deformation process of TENG can be effectively demonstrated through simulations and visualizations. By using animation, one can easily illustrate the working principle of TENG as well as the variations of its potential distribution under different conditions [50]. Additionally, visual distribution maps can provide an intuitive way to present complex physical processes.

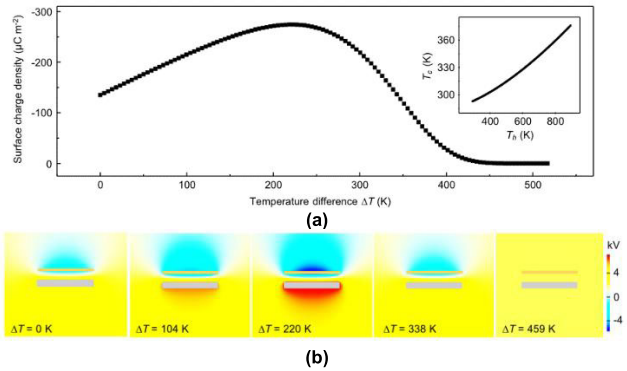

FIGURE 6. (a) Numerical simulations of the relationship between ΔT and the short-circuit transfer charge density. The relationship between the temperature of the hotter friction layer (Th) and the temperature of the cooler friction layer (Tc) is shown in the inset. (b) The potential distribution of TENG under different ΔT [48].

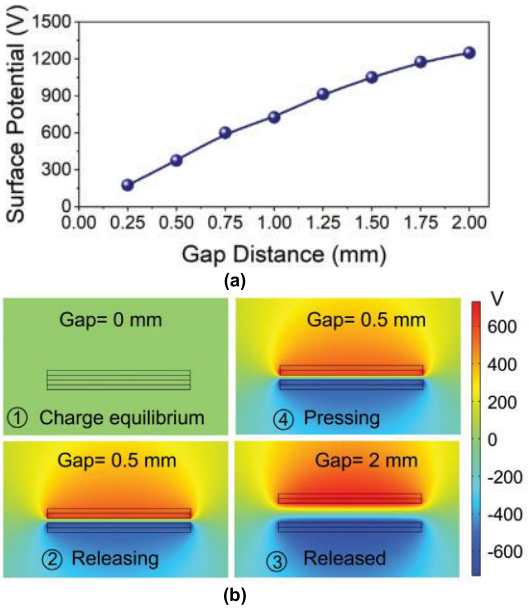

FIGURE 7. (a) The plot of the simulated surface potential of the TENG at various gap distances between the triboelectric pairs. (b) The COMSOL simulation of the TENG [49].

Wu et al. [51] designed a vertical Contact-Separation Mode TENG. To better understand its principles and performance, they used Comsol Multiphysics to perform theoretical simulations of the TENG. Theoretical analysis was conducted through simulation of the electric potential distribution, charge distribution, and energy of the TENG structure, and the simulation results were obtained, as shown in Figure 8. Analysis of the results shows that the electric potential (open-circuit voltage) increases with the increase of the Triboelectric layer spacing, which confirms the electrical principle of the TENG.

The use of simulation software for multiphysics simulation of triboelectric nanogenerators (TENGs), coupled with parameter optimization by adjusting factors such as dielectric constants and charge transfer rates, offers an effective approach to optimize TENG design and enhances its power generation efficiency. The coupling simulation of multiple physical fields accelerates the research process and reduces costs.

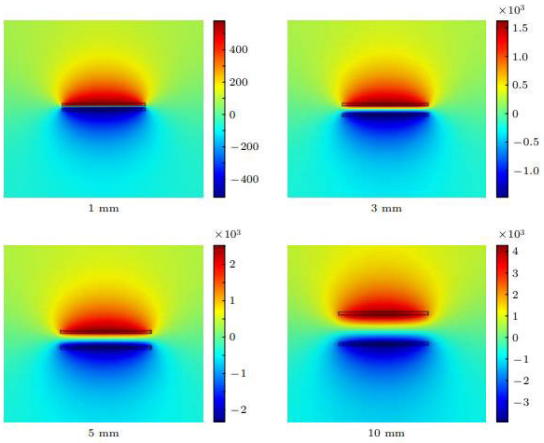

FIGURE 8. The potential distribution picture with different distances [51].

B. SELECTION OF TRIBOELECTRIC LAYER MATERIAL

Considering the application of TENG in robotic hands, TENG-based sensors require high tensile and compliance properties. Therefore, the selected Triboelectric material should exhibit excellent flexibility and pliability.

Negatively charged materials such as polydimethylsiloxane (PDMS) [52], [53], polytetrafluoroethylene (PTFE) [54], [55], [56], fluorinated ethylene propylene (FEP) [57], [58], and polyimide (PI) [59], [60], [61] have been tested for this purpose. PDMS is a promising material for TENG triboelectric layers due to its excellent flexibility and high transparency [62]. In 2012, Fan et al. [63] created micro/nano-patterns on the surface of PDMS using a silicon template, resulting in a transparent TENG with 50% transparency that could be attached to the surface of a mobile phone screen for energy harvesting and pressure detection. The TENG's performance was improved by over three times compared to TENGs without surface patterns, greatly enhancing the sensitivity to induced pressure. In 2016, Zhao et al. [64] utilized sandpaper templates to create surface micro/nanostructures on PDMS and assembled a TENG with a fabrication method that was both simple and low-cost. The output performance of the TENG was improved to more than five times that of a planar PDMS-based TENG, with an output power density of 62.3μW/cm2.

Shi et al. [65] designed a functional sensing element with a micro-structured PDMS layer, using stretchable polymer PET as the substrate and embedding four AgNWs electrodes on the four sides (Fig. 9a). They studied the contact position and velocity of objects detected by simulating intelligent skin, achieving a resolution of up to 1.9mm.

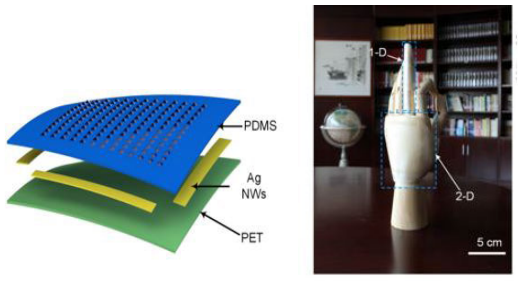

FIGURE 9. (a) Schematic diagram of an analog smart skin. (b) Photograph of an artificial hand covered by two-dimensional analog smart skins on the curved back of the hand and one-dimensional analog smart skins on the middle finger [65].

He et al. [66] developed a flexible unipolar TENG consisting of an oxide/PDMS thin film. The authors conducted a systematic study on the effects of MXene content and compression force on the device's output performance and achieved a peak open-circuit voltage of 225V by periodically manually striking a flexible TENG measuring $2 \times 4\text{cm}^2$.

Additionally, PTFE is widely recognized as an excellent material for the triboelectric layer. In a study by Shankaregowda et al. [35], a graphite-coated paper was used as an electrode, and a PTFE film strip was used as a triboelectric layer to produce a highly flexible single-electrode mode TENG. The device generated a maximum open-circuit voltage of 320 V through hand tapping to collect energy. In another study, Dudem et al. [67] utilized a soft printing process to create microstructures on a silk fibroin membrane to fabricate a vertical contact-separation mode TENG (AT-MASF TENG), with methanol-treated microstructured silk fibroin serving as the positive triboelectric layer and PTFE as the negative triboelectric layer. The sensor generated an impressive output voltage of 395V and a current density of 89 mA/m2. Fig. 10 illustrates the application of the AT-MASF TENG in powering various electronic devices and sensing human body movements.

Yao et al. [68] developed an electronic skin for mechanical hand sensing, leveraging the excellent characteristics of two materials integrated into the same sensor, as depicted in Fig. 11(a). The electronic skin comprises four layers: a shielding layer, a microstructured PDMS layer with silver nanowires (AgNWs) serving as the triboelectric layer, another triboelectric layer comprised of micro-spikes on the surface of microstructured PTFE, and a back electrode layer that interlocks with the upper triboelectric layer. The sensitivity of the pressure measurement was enhanced by 14 times. Fig. 11(c) demonstrates the outstanding tactile sensing ability of the TENG electronic skin sensor by displaying the handshake pressure and bending angle of each finger of a bionic hand when shaking hands with a human. Sun et al. [69] developed a TENG-driven and controlled soft robot called TENG-bot. They proposed a soft robot consisting of a unidirectional dielectric elastomer actuator (DEA), a flexible arch, and a

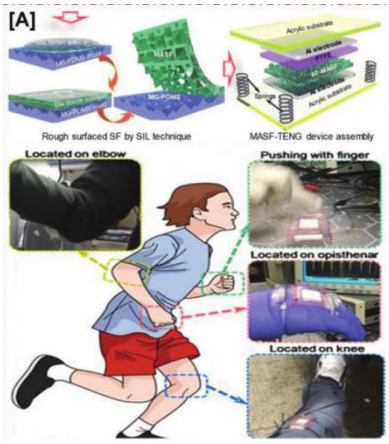

FIGURE 10. Flexible AT-MASF-TENG device to sense various human activities by locating it on different places of the body, i.e., under the finger, on the elbow, opisthenar of hand, and knee, respectively [67].

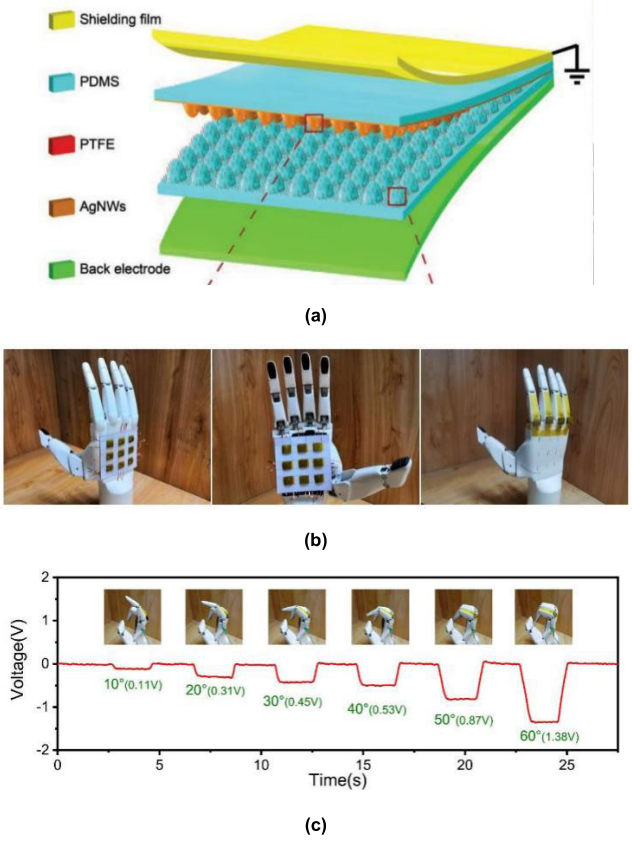

FIGURE 11. (a) Schematic diagram of the TENG e-skin sensor structure. (b) Photograph of 3 × 3 triboelectric sensor arrays attached on the back and palm of a bionic hand, and the TENG e-skin sensors mounted on the finger joints of the bionic hand. (c) Voltage signals in response to index finger gestures with different bending angles after relative humidity of 70% [68].

unidirectional bearing wheel, as shown in Figure 12. For the TENG fabrication, they selected a 25μm-thick FEP film as the sliding part, with two copper electrodes as the fixed part, mounted on an acrylic acid substrate. To enhance the output

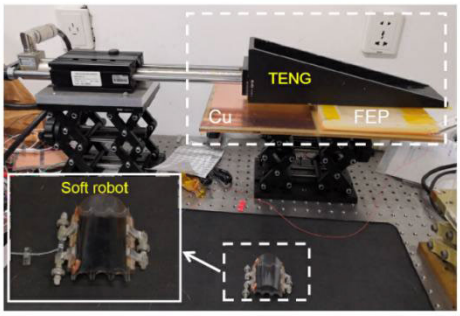

FIGURE 12. An independent TENG is directly connected to a soft robot, generating a voltage when the TENG slides. The voltage drives the DEA (Dielectric Elastomer Actuator), causing the DEA to elongate and contract, resulting in the displacement of the robot. In a sliding cycle, the soft robot completes one motion step [69].

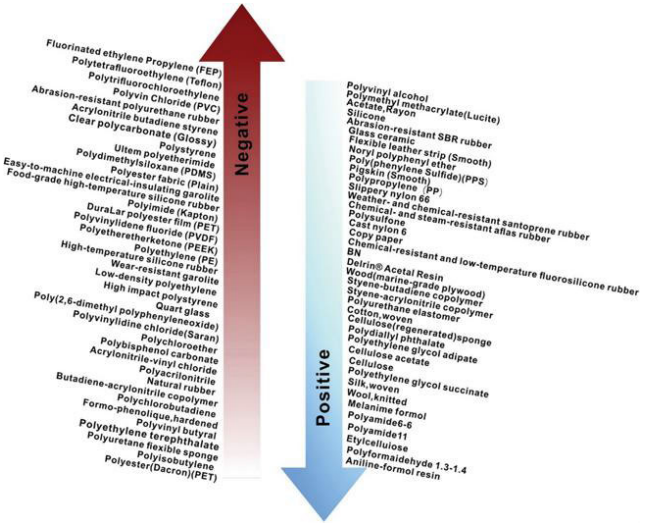

FIGURE 13. The triboelectric series is divided from the most negative tribopolarity to the most positive tribopolarity [73].

performance of the TENG, the bottom surface of the FEP film was treated with inductively coupled plasma (ICP) to form a nano-rod structure [70]. Under no load conditions, a good linear relationship was observed between the motion speed of the soft robot and the sliding speed of the TENG, which is of significant guidance for the power and control of the robot.

Research has demonstrated that PDMS is highly flexible and can be easily processed into various shapes and sizes while also possessing strong adhesion to most substrate materials, such as silicon and glass. Additionally, it is simple to prepare [71]. PTFE, on the other hand, exhibits a high coefficient of friction, excellent wear resistance, and corrosion resistance [72]. Fig. 13 depicts the triboelectric series of TENG materials [73] and illustrates the trend of materials gaining or losing electrons. Materials with positive charges are more prone to losing electrons, whereas negative materials exhibit the opposite effect. There are neutral substances located in the middle of this series, which do not exhibit a strong tendency to attract or lose electrons. As the distance between materials increases, the transfer of charge between them also increases. Therefore, When the top material rubs against the bottom material, there will be more charge transfer. The output power of a TENG can be significantly enhanced by carefully selecting the appropriate material composition, surface roughness, surface potential, and motion parameters and accounting for environmental factors such as humidity and temperature effects.

C. DESIGN AND OPTIMIZATION OF TRIBOELECTRIC LAYER

The TENG's performance is directly related to the charge density of the contact surface. As a result, increasing charge production has consistently been a critical strategy for enhancing output power [68], [72]. The design of the triboelectric layer is centered on the material's micro-structured surface and its functionalization. The micro-structuring of materials can be achieved through a variety of methods, including the assembly of colloidal arrays [74], soft lithography [75], self-assembly of block copolymers (BCP) [76], and surface nano-material manufacturing [77]. These techniques increase the contact area between materials, enhancing the triboelectric effect and improving the detection sensitivity, detection limit, and detection range of sensors. For instance, Fan et al. [63] demonstrated a TENG pressure sensor by fabricating a pyramid-shaped micro-structured PDMS film on the triboelectric layer, which improved performance by 5-6 times compared to non-structured films. Similarly, Yang et al. [78] developed a TENG-based sensor with micro-pyramid-structured PDMS thin films for collecting biomechanical energy and detecting pressure. The research induced a higher charge density through micro-pyramid structures prepared by etching silicon surfaces, resulting in an improved sensitivity of 0.29 ± 0.02 V/kPa. Moreover, micro-pyramid structures can improve surface wettability, providing TENGs with self-cleaning functionality. Man et al. [79] designed a single-electrode TENG (S-TENG) with PDMS as the triboelectric layer and microscale relief structures on the surface. A 20nm thick indium tin oxide film was used as the electrode layer, and external circuits were used to output electrical energy. The microscale relief structure improved the electrical performance of the triboelectric layer. The open-circuit voltage and short-circuit current of the S-TENG were detected by applying different external pressures, and the results showed that the open-circuit voltage of the prepared S-TENG reached 80V. Jeong et al. [76] demonstrated a novel TENG design concept using nano-patterning technology and BCP self-assembly. By controlling the self-assembly of polystyrene-block-polydimethylsiloxane (PS-b-PDMS) thin films, various silica nanostructures, including nanodots, nanogrates, and nanomeshes, were achieved. The silica film with the nanostructure, combined with polytetrafluoroethylene, effectively generated electricity. The BCP-TENGs with nanostructures exhibited significantly improved output performance, with voltage and current densities of up to 130 V and 2.8 $mA{\cdot}m^{-2}$, respectively.

In conclusion, the triboelectric layer's microstructure plays a crucial role in enhancing the performance of TENG-based sensors. Various methods can be used to achieve the desired microstructure, such as assembling colloidal arrays, soft lithography, self-assembly of block copolymers, and surface nano-material manufacturing. These methods increase the contact area and improve the Measurement accuracy, detection limit, and detection range of sensors. The micro-pyramid structure is a popular design choice that can improve surface wettability, provide self-cleaning functionality, and extend the lifespan of TENGs. However, the most suitable microstructure should be selected based on the specific application to achieve more accurate and reliable measurements and detections.

The functionalization of materials can be achieved through various methods, such as ion doping, plasma treatment, polarization, laser induction, and the formation of nanocomposites [80], [81], [82], [83], [84], [85] In TENGs, materials such as BaTiO3, TiO2, graphite, graphene, ZnSnO3 nanocubes, and PTFE have been used as dopants in PDMS to improve output performance [86], [87], [88], [89], [90], [91]. Jing et al. [92] proposed a method to improve the triboelectric performance of PDMS composite materials by filling the PDMS matrix with high dielectric constant liquids, which can reduce the effective thickness of PDMS while increasing the dielectric constant of the PDMS composite material. When the filling ratio is 50% (PDMS-hd50), the triboelectric properties are improved by 4.5 times the output voltage and 3.9 times the output current compared to pure PDMS.

Fluorine-containing elements with the strongest electronegativity are typically chosen as triboelectric materials in TENG design [93]. Matsunaga et al. [94] modified the surface of PDMS with carbon tetrafluoride plasma and used spray technology to prepare a large area (12 × 12 cm) S-TENG for wearable energy harvesting (Fig.14(b)), increasing the output power to 8 W/m2. Li et al. [95] introduced F elements by adding FDTS to PDMS and fabricated a flexible PDMS-FDTS film as a negative triboelectric layer. A 4 cm2 TENG was made using PET as the positive triboelectric layer and copper nanowires/reduced graphene oxide (Cu-NWs/RGO) as the electrode. It had an output voltage of 125 V.

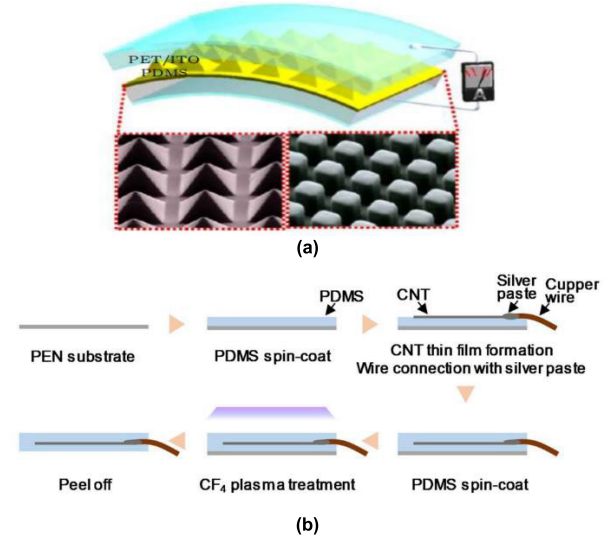

FIGURE 14. a. Nanowires and Pyramid arrays [63]. b. Schematic of fabrication procedures of S-TENG [84].

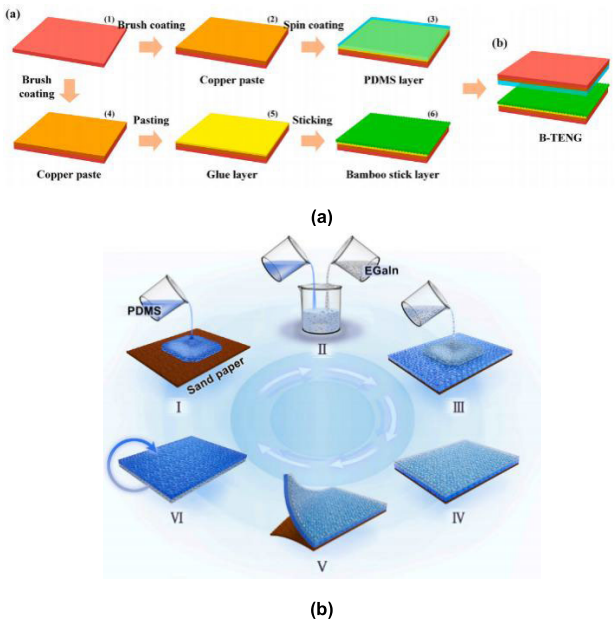

FIGURE 15. (a) . (a1-a5) The fabrication process of the PDMS layer and bamboo stick layer [96]. (b). The fabrication process of the self-powered triboelectric tactile sensor with PDMS/EGaIn alloy electrode [97].

D. THE FABRICATION OF TENG

The fabrication method for TENG depends on the specific design and choice of materials. The coating is a general fabrication method for TENG, where the basic idea is to coat the triboelectric layer and electrode on the substrate, then apply a sealing layer on the electrode to form a closed structure. This method can quickly fabricate TENG and adapt to different substrate materials and size requirements. Ding et al. [96] first cut polyethylene and spun a layer of PDMS on the surface of copper foil to form a PDMS triboelectric layer. The conductive copper foil was then attached to the surface of another substrate, as shown in Fig. 15(a4). A layer of glue was coated on the surface of the copper foil, as shown in Fig. 15(a5). Glued onto the surface of the glue as shown in Fig. 15(a6). Finally, the two parts were combined to form a B-TENG. In another study, Wang et al. [97] used a coating method to fabricate a self-powered TENG-based tactile sensor with a multilayer PDMS triboelectric layer and a PDMS/eutectic gallium-indium (EGaIn) composite electrode. The sensor (Fig. 15(b)) achieved a detection limit of 7 mPa.

Wang et al. [98] employed spin-coating to apply a layer of PDMS onto a mold, and subsequently utilized a solution comprising silver nanowires (AgNW) for spraying onto the

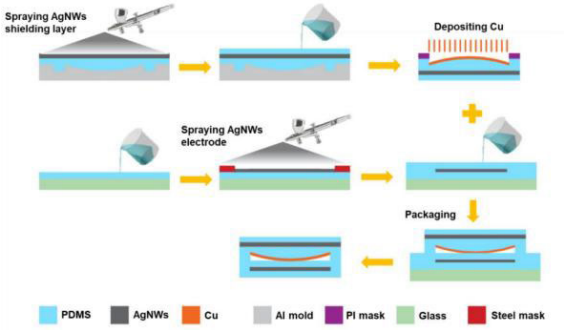

FIGURE 16. Fabrication processes of the TENG E-skin pressure sensor [98].

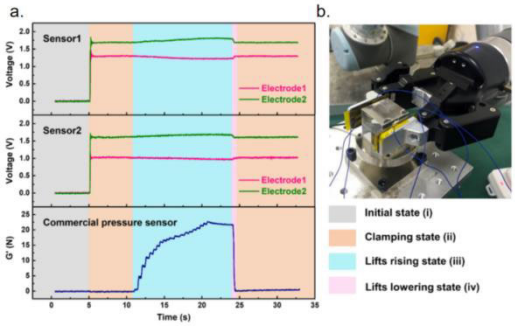

FIGURE 17. (a) The output VOC of sensor 1, sensor 2, and the shear force measured by a commercial pressure sensor during the whole process. (b) Applications of the TENG E-skin multi-dimensional force sensor in tactile sensing during robotic manipulation [98].

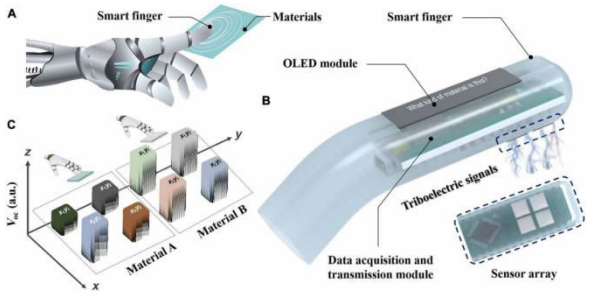

FIGURE 18. (a) Schematic diagram of the material identification process of the triboelectric tactile perception smart finger. (b) Structure of the triboelectric tactile perception smart finger, consisting of a triboelectric sensor array, data acquisition and transmission module, and display module. (c) Schematic diagram of the output signals of the triboelectric sensor array when the smart finger identifies different materials. a.u., arbitrary units [99].

PDMS surface, serving as a shielding layer for the electrodes. Another layer of PDMS was applied for surface encapsulation, and a copper (Cu) film was deposited on the curved structure of the PDMS as a flexible friction layer for contact and separation. Then, PDMS was spin-coated on a glass substrate and baked, followed by spraying a solution containing silver nanowires (AgNW) on the PDMS surface and applying a layer of circular patterned electrodes. A conductive silver paste was used to attach conductive tape on the electrodes, and another layer of PDMS was spin-coated on top. Uncured PDMS was applied around the top layer, bonding the top and bottom layers together, followed by baking. The fabrication process is illustrated in Figure 16. Figure 17 shows the application of the TENG-based multidimensional force sensor (TENGe-skin) in tactile sensing during robot manipulation. Qu et al. [99] developed an intelligent finger that surpasses human tactile perception for material type and roughness recognition in prosthetics and robotic hands. The intelligent finger integrates sensor arrays, a signal acquisition module, a processing module, a communication module, and an OLED screen. The sensor array consists of four TENGs, each adopting high-purity materials: PA66, PET, PS, and PTFE films as the friction layers, with aluminum foil coated as the friction layer on the surface of high-purity materials. The size of the sensors is 1×1 cm^2. The housing of the intelligent finger is 3D-printed. The sensor array is integrated beneath the fingertip, as shown in Figure 18(b). This intelligent finger can be integrated into smart prosthetics or robotic hands and can recognize various textures such as polymers, metals, and wood.

Zhang et al. [32] demonstrated how to fabricate a multifunctional electronic skin sensor using a spin-coating technique. A layer of silver nanowires (AgNWs) solution in ethanol was first spin-coated onto a glass substrate, followed by a layer of polydimethylsiloxane (PDMS) and curing agent mixture, which was then vacuum-dried and cured. The resulting film was peeled off, and a copper foil was attached to its surface. Another layer of PDMS was spin-coated on top to form the triboelectric layer, and PDMS surface microstructures were created. The sensor was prepared by mixing PDMS, curing agent, zinc sulfide, and Cu fluorescent powder. Moreover, Yao et al. [68] fabricated a flexible electronic skin by casting uncured PDMS onto a microstructured template, followed by vacuum placement to eliminate bubbles and peeling the microstructured PDMS substrate from the template after an hour of curing. The PDMS substrate had a surface of polytetrafluoroethylene tinny burrs, and the flexible electrode was made of an AgNWs network. The fabrication process of the flexible electronic skin is shown in Fig. 19(b).

The coating method is a widely used and cost-effective technique for fabricating TENGs. However, the substrate material and coating quality can limit TENG performance. In addition to the coating method, He et al. [1] used the doctor-blade method to fabricate a sandwich-structured TENG. Fig. 20 shows that TENG-based sensors capable of rapid self-healing at a specific temperature were equipped. The self-healing polymer material NBR was dripped onto the bottom plate and scraped into a thin film using a scraper to form the first layer. Then, the second layer was formed by spraying a coating of MXene onto the first layer of NBR. Several drops of NBR material were dripped again, and the NBR was scraped into a thin film to form the third layer. Since self-healing materials were used, the triboelectric layer and conductive layer could be repaired within 5 seconds by

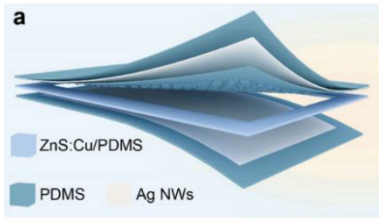

(a)

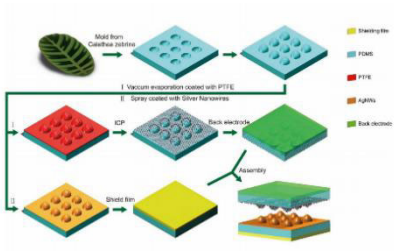

(b)

FIGURE 19. (a) Structure schematic depiction of the STMES [32]. (b) Schematic fabrication processes of the TENG e-skin sensor [68].

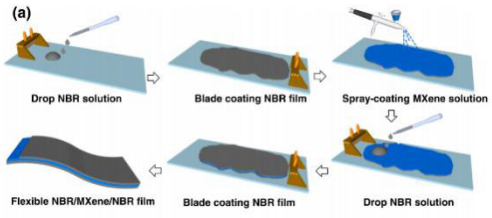

(a)

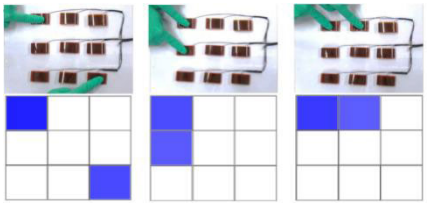

(b)

FIGURE 20. (a) The fabrication process and structure of the NBR/MXene/NBR film. (b) The sensor array and corresponding recorded mapping images when two tactile sensors were simultaneously triggered [1].

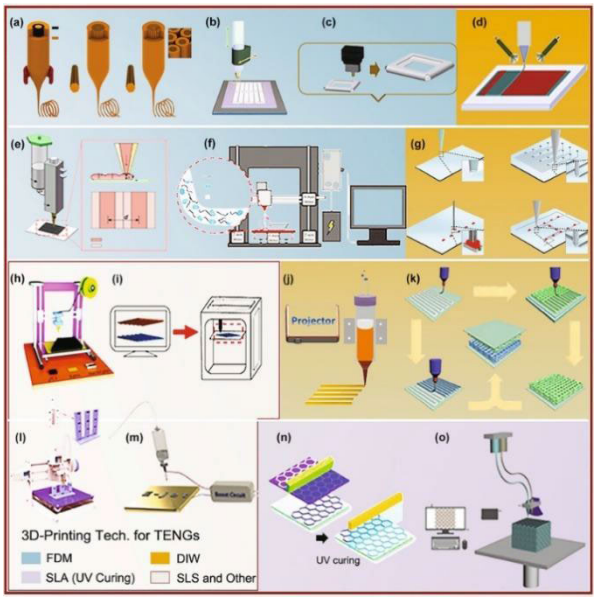

FIGURE 21. Schematic illustrations and structure demonstrations of 3DP-based TENGs by various 3DP technologies [100]. (a) ,(b),(c),(e) and(f) Schematic illustrations and structure demonstrations of 3DP-based TENGs by FDM technology [76], [101], [102], [103], [104], [105], [106], [107], [108], [109], [110], [111], [112], [113], [114]. (d),(g),(j),(k) Schematic illustrations and structure demonstrations of 3DP-based TENGs by DIW technology [76], [106], [107], [108]. (h),(i),(l),(m) Schematic illustrationsand structure demonstrations of 3DP-based TENGs by SLS and other technologies [110], [111], [112], [113]. (n) and (o) Schematic illustrations and structure demonstrations of 3DP-based TENGs by SLA technology [109].

heating with a hair dryer. This approach could improve the durability and performance of TENGs, making them more suitable for practical applications.

In addition to the coating method, 3D printing (3DP) technology has also been utilized to fabricate TENGs [100]. As shown in Fig. 21, various 3DP techniques such as fused deposition modeling (FDM) [101], [102], [103], [104], [105], direct ink writing (DIW) [76], [106], [107], [108], stereolithography (SLA) [109], and selective laser sintering (SLS) [110], [111], [112], [113] have been employed. However, other 3DP techniques, such as photolithography and plating, are rarely used [114]. These researches have shown that FDM technology is particularly suitable for fabricating longer and thinner filamentous films [102], [103] and array structures [104], [105] with significant economic benefits, making it a promising method for the design and development of new triboelectric materials.

Although the coating method is currently widely used in the fabrication of TENG-based sensors, with the advancement of technology and considering issues related to the accuracy, it is believed that the future of TENG fabrication will rely heavily on 3D printing technology. This method offers excellent potential for producing customized and complex TENG structures with enhanced performance and durability, thus opening up new possibilities for practical applications. The aforementioned methods can be selected based on specific requirements and adjusted according to different structures and materials. It is essential to choose suitable materials, design appropriate structures, accurately control the thickness and size, and ensure a clean fabrication process to obtain efficient and stable TENGs. By doing so, achieving the desired performance and durability is possible, thus enabling TENGs to be effectively applied in various fields.

IV. APPLICATIONS OF TENGs ON THE MANIPULATORS

There has been extensive research on incorporating Triboelectric Nanogenerator (TENG) sensors into robot arms, with

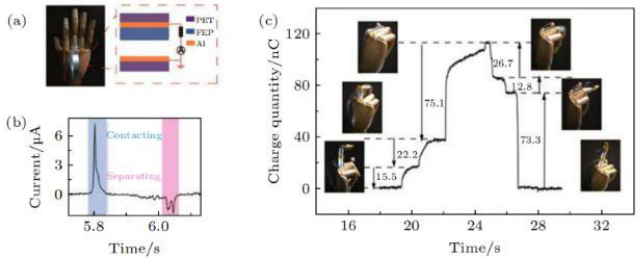

FIGURE 22. (a) A digital photograph and schematic diagram of the TENG combined with the artificial hand. The bending and straightening movement of the finger causes contacting and separating states of the TENG. (b) The reversed current signal in one process of contacting and separating. (c) Transferred charge quantity curve of different random movements of the middle finger [125].

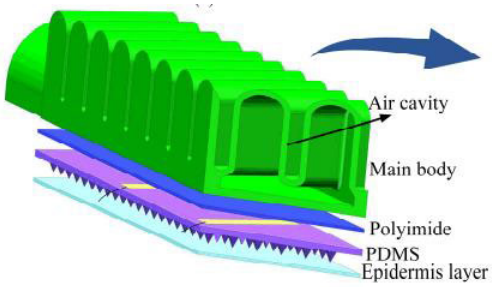

FIGURE 23. The structure of the soft gripper integrated with a TENG-based tactile sensor [126].

a primary emphasis on both self-powered sensing [115] and data communication [116]. Recent studies in this field are summarized in Table 3.

A. TACTILE PERCEPTION

TENG-based tactile sensors technology has been developed for robotic hands to enhance external object perception and recognition, leading to more accurate human-machine interactions. In a study by Jin et al. [125], a self-powered motion detection sensor with a fluorinated ethylene propylene triboelectric layer and an aluminum film electrode was created. An electric signal was produced during contact separation when the sensor was attached to the hand (Fig. 22(a)). Fig.22(b) shows that the device can convert mechanical energy generated by finger movements into electrical signals. During complex and random movements of fingers, the contact areas between the sensor and the upper, middle, and lower joints vary. This variability enables the identification of which joint or joints were moved by analyzing the magnitude of the signal, as shown in Figure 22(c).

Li et al. [126] applied TENG tactile sensors in a soft robot gripper for object shape recognition. The gripper design(Fig. 23) incorporates four TENG electrodes to sense pressure. When pressure is exerted on a specific electrode, a voltage signal is generated at that location. When pressure is exerted between two electrodes, adjacent electrodes receive similar signals, enabling rough recognition of the shape of the grasped object. Jin et al. [127] developed an intelligent soft

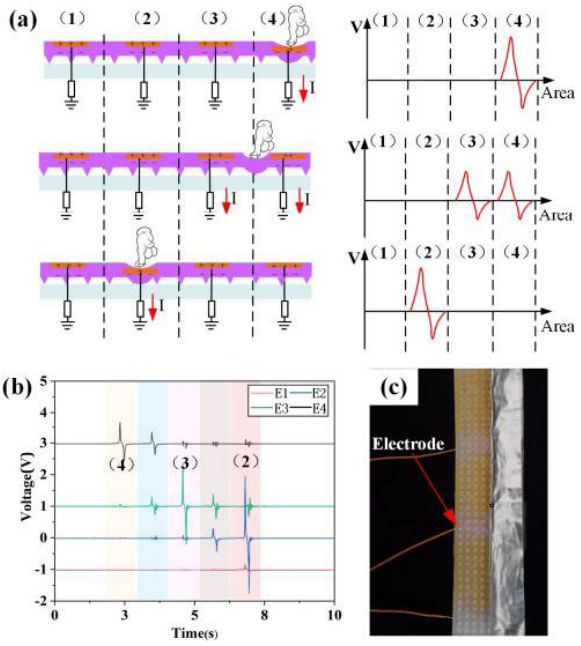

FIGURE 24. The T-TENG test. (a) The ideal output of the four electrodes. (b) The press test of T-TENG from E4 to E2. (c) The T-TENG device [126].

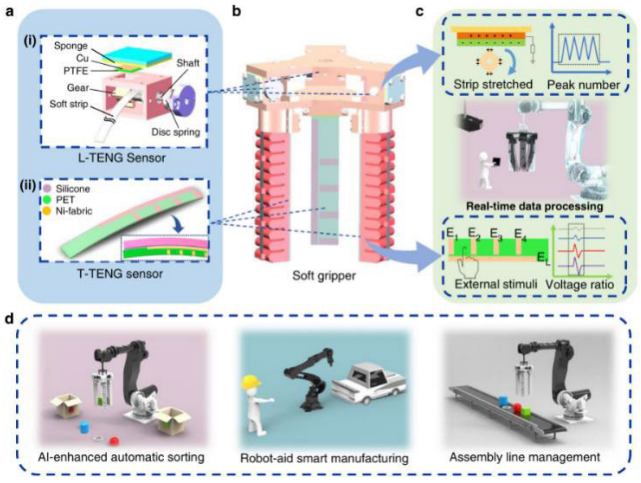

FIGURE 25. (a) TENG Sensor and Its Basic Structures. (i)(i) Length-TENG (L-TENG) sensor and (ii) Tactile-TENG (T-TENG) sensor. (b) A soft gripper integrated with TENG sensors. (c) An intelligent sensory data processing strategy is introduced. E1∼E4, and EL are the electrodes of the T-TENG sensor. (d) a digital twin application based on the AIoT perception system is presented [127].

robot gripper system based on TENG sensors (Fig. 25). The system captures the soft gripper's continuous motion and tactile information. A distributed electrode in the tactile sensor senses the contact position and area of external stimuli. The gear-based length sensor with a stretchable strip allows the continuous detection of elongation via the sequential contact of each tooth. The system can recognize different objects by using the SVM algorithm to train the triboelectric haptic data collected during the soft gripper operation.

TABLE 3. Applications of TENGs on robot arms.

Time	Author	Research content:	Sensing materials	Electrode materials	Device performance.	Sensing Categories
2017	Pu [117]	Ultrastretchable, transparent triboelectric nanogenerator as electronic skin for biomechanical energy harvesting and tactile sensing	PDMS	Graphene	Detect finger movement through touch with a minimum detection pressure of 1.3 kPa.	pressure sensing
2019	Lee [118]	Graphene-based stretchable/wearable self-powered touch sensor	PDMS	Multi-walled carbon nanotubes (MWCNTs)	Pressure range of 1 ~ 40 kPa and capable of accurately detecting finger movements.	pressure sensing
2016	Shi [65]	Self-Powered Analogue Smart Skin	PDMS	AgNWs	The resolution can reach up to 1.9 mm	pressure sensing
2020	He [66]	Flexible single-electrode triboelectric nanogenerators with MXene/PDMS composite film for biomechanical motion sensors	MXene/PDMS composite material	Copper-nickel alloy	Simulating human skin with pig skin, the maximum output of open circuit voltage is up to 170 V, and 20μA cm^{-2} short-circuit current density.	pressure sensing
2021	Wang [99]	A stretchable self-powered triboelectric tactile sensor with EGaIn alloy electrode for ultra-low-pressure detection	PDMS	PDMS/EGaIn alloy composite electrode	The device has ultra-low detection limits and high sensitivity. It has achieved the lowest detection limits of 7 mPa.	pressure sensing
2022	Zhang [119]	Flexible single-electrode triboelectric nanogenerator with MWCNT/PDMS composite film for environmental energy harvesting and human motion monitoring	MWCNT/PDMS thin film	Ag/textile silver textile	Under continuous pressure, the peak open-circuit voltage can reach 435V, and the maximum short-circuit current density is 13 μA·cm2.	pressure sensing
2018	BU [120]	Stretchable Triboelectric-Photonic Smart Skin for Tactile and Gesture Sensing	Ecoflex 00-20	AgNWs	STPS can be used as TENG to sense vertical pressure, with a maximum sensitivity of 34 mV/Pa-1.	pressure sensing
2022	Zhang[32]	Self-powered triboelectric-mechanoluminescent electronic skin for detecting and differentiating multiple mechanical stimuli	PDMS	AgNWs	When used as a contact-separation mode TENG, its maximum sensitivity is 2 V/N.	pressure sensing
2019	Zheng[34]	Dual-Stimulus Smart Actuator and Robot Hand Based on a Vapor-Responsive PDMS Film and Triboelectric Nanogenerator	Nylon and PDMS	Al	The electrostatic force provided by TENG can be used to move or control the target object, and the gripper can hold objects with a weight of up to 6g.	slip force sensing
2018	Xia [121]	A triboelectric nanogenerator as a self-powered temperature sensor based on PVDF and PTFE	PTFE /PVDF	conductive copper foil	The temperature detection range is 10–90 °C and the response time and reset time of the sensor are approximately 0.01 and 3.5 s	temperature sensing
2019	Xiong [122]	Self-restoring, waterproof, tunable microstructural shape memory triboelectric nanogenerator for self-powered water temperature sensor	SMPU mats	Al	The sensitivities of the device are 0.11 V °C−1 and 0.2 V °C−1 at impacting times of 5 s and 10 s, respectively, for the water temperature between 25 ± 5–95 °C.	temperature sensing
2021	Fan [123]	A whirligig-inspired intermittent-contact triboelectric nanogenerator for efficient low-frequency vibration energy harvesting	FEP	Cu	the IC-TENG can be driven by hand, and the tapping operation can empower the IC-TENG to illuminate 120 LEDs	slip force sensing
2021	Nie [124]	A sliding hybrid triboelectric-electromagnetic nanogenerator with staggered electrodes for human motion posture	PTFE	Al	Compared to the dielectric sliding parts, the sliding TENG with a conductive magnet can obtain higher electrical output. The Voc, Isc, and transfer charge of the TENG section of SHTE-NG can arrive at 175 V, 3.25 μA, and 75 nC, respectively.	slip force sensing

Machine tactile perception encompasses various aspects, including not only pressure sensing [65], [66] but also temperature sensing [121], [122] and slip force sensing [123], [124], among others.

The electrical properties of nanomaterials are influenced by temperature, causing changes in the charge distribution within the nanomaterials when in contact with objects of different temperatures. By monitoring these variations in charge distribution, TENGs can convert them into electrical energy and utilize it to perceive the temperature of the object. Xia et al. [121] proposed a self-powered temperature sensor constructed using a TENG. The sensor employed TENG made of polytetrafluoroethylene and polyvinylidene fluoride, with conductive copper foil serving as the electrodes and silicon paper and polyvinylidene fluoride film as the supporting structure, as shown in Figure 26. This TENG was capable of detecting temperature changes within the range of 10 to 90 degrees Celsius, with a response time of 0.01 seconds

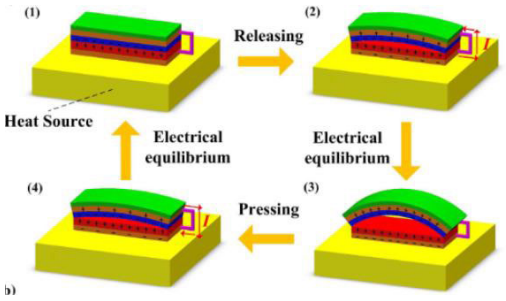

FIGURE 26. The working mechanism of the TENG during one cycle [121].

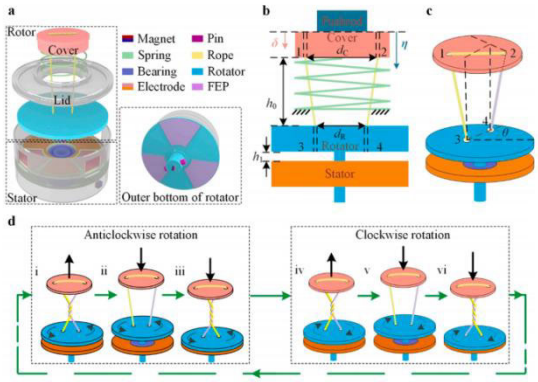

FIGURE 27. (a) Three-dimensional structure. (b) Two-dimensional view. (c) Geometric structure of the rotor with a rotation angle θ. (d) Working principle with the black arrowheads denoting the direction of external excitation [123].

and a reset time of 3.5 seconds. The study also discussed other types of self-powered sensors, including temperature sensors that convert mechanical energy into electrical energy using TENG. These sensors hold potential applications in healthcare, environmental monitoring, energy harvesting, and other fields.

Xiong et al. [122] developed a self-healing, waterproof, and tunable microstructured shape memory triboelectric nanogenerator (TENG) for self-powered water temperature sensing. The TENG was fabricated using shape memory polymers that can recover their original shape from a temporary deformation upon temperature stimulation. The TENG collected energy from both cold and hot water and served as a self-powered sensor to provide real-time indication of water temperature. The article extensively explains the working principle of the TENG: the impact of hot water causes the sensor's microstructure to recover into different forms, resulting in varying voltage outputs that enable temperature sensing of the water. Therefore, this technology can be applied in various scenarios where water temperature measurement is required, such as aquaculture and water resource management fields.

TENGs can also perceive the frictional sliding between objects. In terms of slip force sensing, Fan et al. [123] designed a rotating intermittent-contact triboelectric nanogenerator (IC-TENG) structure, as shown in Figure 27(a). This generator was capable of harvesting low-frequency

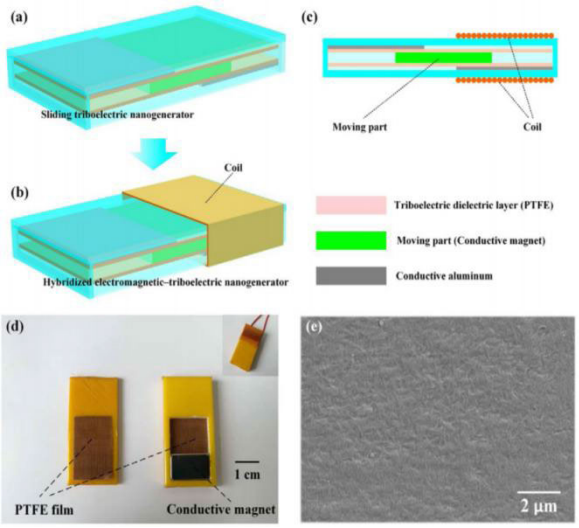

FIGURE 28. (a) The schematic illustration of the sliding triboelectric nanogenerator with staggered electrodes. (b, c) The schematic illustration of the SHTE-NG. (d) The picture of the SHTE-NG. (e) The SEM images of PTFE film surface [124].

vibration energy. The IC-TENG employed a sliding rope to drive the rotor, which initiated rotation through a dynamic mechanism similar to a carousel, converting low-frequency vibrations into the high-speed rotation without the need for manual operation. The IC-TENG exhibited high electrical stability, with its normalized electrical output remaining stable at approximately 81%, while the normalized electrical output of non-contact mode TENG decayed to 48% within 10 days. The IC-TENG holds potential as a sustainable and decentralized energy solution for small-scale low-power electronic devices by harnessing commonly available low-frequency vibration energy.

Furthermore, Nie et al. [124] designed a novel sliding hybrid triboelectric-electromagnetic nanogenerator (SHTE-NG) for harvesting mechanical energy and sensing human motion postures. The SHTE-NG consists of a triboelectric part and an electromagnetic part, with the conductive magnet serving as the frictional material. The triboelectric part and the electromagnetic part are connected through a rectifier bridge to collect mechanical energy and generate electrical output. The structural diagram is shown in Figure 28. The authors installed the SHTE-NG on the human leg to sense human motion states and reflected different motion states through different electrical signals generated by the triboelectric part. The article also presents detailed output results of the electrical signals generated by the TENG part under different motion states. This demonstrates that the SHTE-NG can serve as a self-powered human motion posture sensor to reflect different motion states.

Through these tactile sensing capabilities, triboelectric nanogenerators can achieve the perception of external objects' pressure, temperature, and frictional sliding infor-

mation. This technology holds potential applications in fields such as biomedicine, robotics, and wearable devices.

Electronic skin sensors possess multimodal also sensing capabilities, enabling them to detect and monitor a variety of stimuli, including distance, pressure, strain, temperature, and more. They can even monitor multiple stimuli simultaneously [128], [129], [130]. Unlike traditional sensors that rely on rigid substrates and functional materials, the flexibility and stretchability of electronic skin sensors present unique challenges in terms of TENG materials, structural design, and fabrication methods [131], [132]. Along with their self-powering properties, measurement sensitivity is crucial for electronic skin sensors to emulate the perceptibility of human skin. TENG-based sensors' sensitivity and measurement range can be enhanced or adjusted by altering surface conditions, device modes, or structures [133], [134], [135], [136], [137].

Pu et al. [117] have developed a flexible and transparent TENG (Fig. 29) that employs an elastic body and ion hydrogel as the charged layers and electrodes. The design enables the device to harvest biomechanical energy and enable tactile sensing while still maintaining high stretchability and transparency. As a result, these TENGs are well-suited for powering wearable electronic devices.

Due to their high sensitivity to pressure, STENGs are suitable for touch/pressure sensing in artificial electronic skin. Yao et al. [68] fabricated interlocking structures in the triboelectric layers by replicating the cone-like array microstructures of the Calathea zebrine leaf. The chained microstructure and production of PTFE micro protrusions significantly increase the triboelectric effect. The self-powered electronic skin developed was applied to a bionic hand, and the tactile sensing ability of the TENG-skin sensor was demonstrated by measuring the distribution of gripping pressure and bending angle for each finger of the bionic hand. Additionally, the authors conducted a 5000-cycle loading test under a pressure of 25 kPa, and the sensor output remained stable, demonstrating the high durability of the sensor. Wang et al. [33] have reported a self-powered large-area integrated TENG array (TSA) that used a TENG array and a CD4066 array chip connected through traditional coupling (Fig. 30). This TSA can detect static and dynamic pressures, and its ground shielding layer suppresses crosstalk, effectively solving the problem of crosstalk signals. The TSA has been integrated with signal processing circuits to create a complete wireless sensing system. Bu et al. [120] have developed a stretchable triboelectric-Photonic Smart Skin (STPS) for a robotic hand. The STPS(Fig. 31) allows for multidimensional tactile and gesture sensing. It adopts a single-electrode mode to sense external touch and vertical pressure, using silicone rubber as the triboelectric layer and Ag NWs as the stretchable electrode. The surface of the silicone rubber has been treated with sandpaper to create a microstructure. The grating structure of metal film serves as the biological excitation skin stripe, enabling STPS to exhibit tunable aggregation-induced emission within a lateral

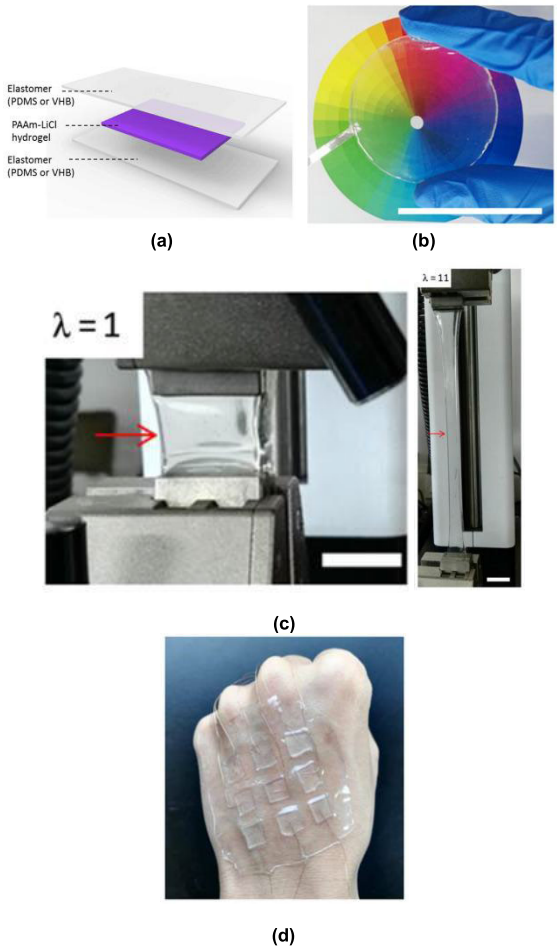

FIGURE 29. a) Scheme of the STENG with sandwich structure. (b) A circular STENG transparent to full visible colors. (c) VHB-STENG (indicated by arrows) at initial state (stretch l = 1) and stretched state (l = 11 or strain e = 1000%). (d) An image of a STENG-based tactile sensor with 3 × 3 attached to a curvy hand [117].

stretch range of 0-160%. As the tensile strain increases, the brightness significantly increases.

Additionally, researchers have combined TENG-based sensors with other types of sensors to improve their sensing capabilities. For example, Yuan et al. [138] developed a sensing device that combines a capacitive-type transducer with a TENG-based sensor. This device is designed for flexible manipulators and can achieve high sensitivity and intelligent recognition of grasping force. The capacitive transducer is used to identify pressure and deformation, while the TENG part senses sliding motion, the linear relationship between the displacement of the contacted object, and the transferred charge. Furthermore, The peaks in current signals can also indicate the sliding velocity of the contact object. This combination provides a method to avoid accidental sliding and damage during the flexible grasping process.

Another example is the hybrid energy harvesting method proposed by Zhu et al. [139], which combines piezoelectric and triboelectric methods. They fabricated a composite

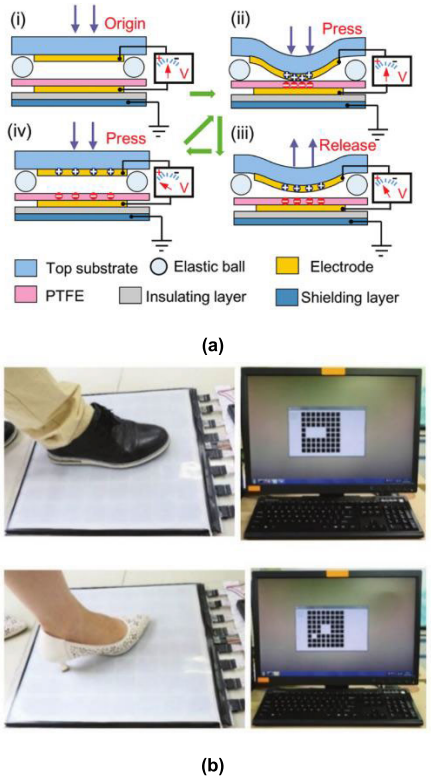

FIGURE 30. (a) The working principle of the TSA. (b) Wireless foot-stepping experiments conducted with a leather shoe and a heel [33].

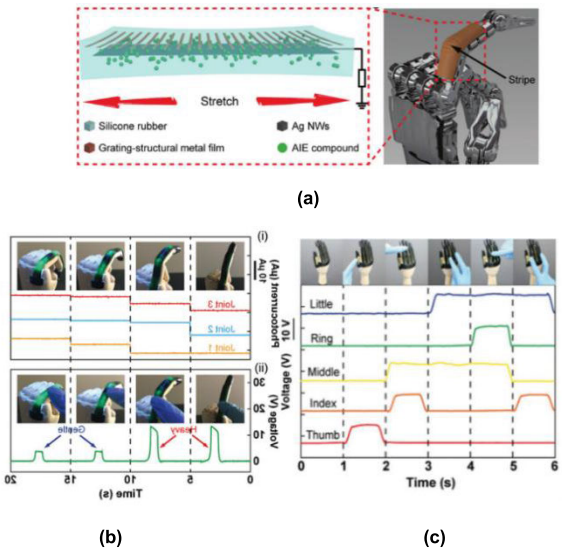

FIGURE 31. (a) Schematic diagram of the structure of STPS and Schematic diagram of the STPS for a robotic finger. (b) Open-circuit voltages of STPS with different touching conditions by a human hand, which are shown in upside photographs. (c) The photocurrent (i) excited by PL of STPS through bending the finger with different states, and the synchronous open-circuit voltages (ii) by touching the different areas of STPS [120].

material of PVDF/PTFE composite film and triboelectric leaf-shaped micro-structured film. The design of PVDF nanoparticles and leaf-shaped woven fiber PTFE film enhances the collection efficiency of the composite film,

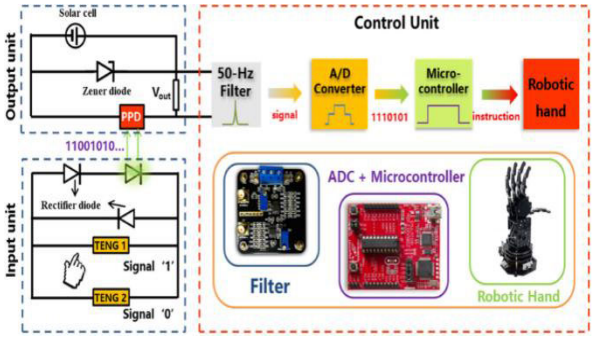

FIGURE 32. Circuit of diagram of SOCS and control unit. The tapping signals can be transmitted and converted into instructions for a robotic hand [148].

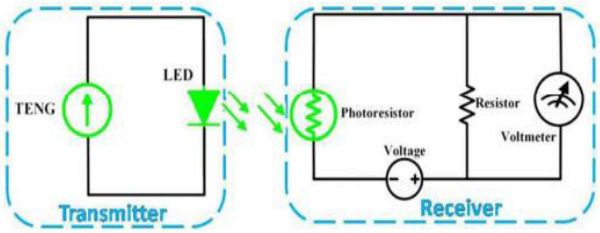

FIGURE 33. Schematic diagram of a communication system based on the TENG as a self-powered communication unit [116].

while the designed leaf-shaped PTFE film enhances the power output of the TENG.

B. DATA COMMUNICATION

The development of self-powered TENG sensors [21], [140], [141], [142], [143], [144] has opened up possibilities for designing self-powered communication systems that can convey information from people or objects. For such communication systems, information recognition and signal transmission are critical functions. TENG devices can respond to different frequencies and produce unique output performance under vibration excitation due to the resonance phenomenon [145], [146], [147]. This property may help establish working bands for selectively recognizing special signals to transmit information.

Guo et al. [148] proposed a self-powered organic light communication system (SOC) (Fig. 32). The system consists of organic light-emitting diodes driven by TENGs and perovskite photodetectors provided by solar cells. Due to the excellent performance of the optoelectronic coupler, SOC can effectively convert mechanical signals into optical signals and then into voltage signals between two insulated units, synchronously realizing information transmission. The system encodes the mechanical tape of different areas of TENGs into binary, enabling large amounts of data transmission and successfully controlling the mechanical hand to complete different actions. It reflects the intelligent application of SOC in human-machine interaction. Yu et al. [116] designed a self-powered communication unit based on TENG

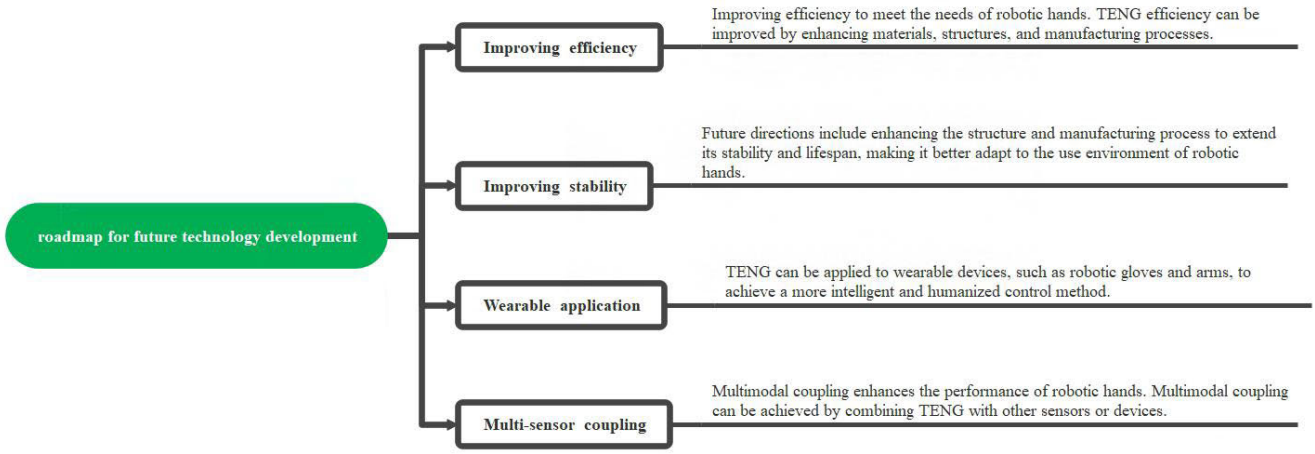

FIGURE 34. The roadmap for future technological developments.

(Fig. 33). The TENG works in different frequency regions, collecting specific frequency environmental trigger signals as the energy supply of the entire communication system. The collected trigger signals can also be converted into binary digital signals and transmitted directly by optoelectronic devices without external power. The elaborately designed TENG is built in a membrane structure, which can effectively drive electronic-optical devices within a bandwidth of 1.30 kHz to 1.65 kHz. In addition, A design based on cantilever structures, driven by low-frequency vibration signals in the frequency range of 16∼22 Hz, further demonstrates the ability and feasibility of TENG technology for information communication. The design flexibility of the TENG technique allows for transmitting triggering signals at various frequencies.

Therefore, The TENG design can function as electronic skin attached to a manipulator for improving precision, stability, and performance. It can also provide bidirectional feedback between the robot's end effector and control system, similar to human palm touch and nerves, enabling precise control [149]. TENG technology has substantial prospects in human-machine interaction, soft robotics, and artificial intelligence fields.

V. CONCLUSION

In recent years, TENG has made significant breakthroughs and developments as both a power generator and a sensor, demonstrating its potential for various applications. To further enhance its application in robotic hands, the roadmap for future technological developments is as follows:

Significant progress has been made in synthesizing and selecting materials, device fabrication schemes, and the performance of flexible sensors based on TENG. However, to achieve practical applications of TENG-based self-powered sensors, particularly in robotics, challenges still need to be addressed.

1) TENG-based pressure sensors are sensitive in a low-pressure range, and the sensitivity decreases with increasing pressure, limiting the measurement range. New solutions, such as the design of layered stiffness materials and structures, need to be explored.
2) Multimodal and high spatial resolution sensing has great appeal for robotics, but the static interference between adjacent TENG unit cells and interconnections can significantly affect measurement accuracy, especially in a large array of sensor units. Integrating a shielding layer in the device has been proven to eliminate interference effectively, but additional components must be balanced to maintain device complexity.
3) To achieve touch sensing capabilities similar to humans, TENGs must be combined with other mechanisms to achieve multifunctional sensing. For example, the human sense of temperature is a critical element of touch sensing, but the mechanical motion or force that triggers TENGs sensors cannot measure temperature. Recent efforts to integrate thermoelectric materials in sensor arrays represent promising steps in this direction.
4) Prolonged mechanical impacts and harsh working environments, such as high temperatures and humidity, challenge the robustness and reliability of sensors. Therefore, researchers must develop robust and reliable sensors that can withstand such environments.

REFERENCES

[1] W. He, S. Li, P. Bai, D. Zhang, L. Feng, L. Wang, X. Fu, H. Cui, X. Ji, and R. Ma, "Multifunctional triboelectric nanogenerator based on flexible and self-healing sandwich structural film," *Nano Energy*, vol. 96, Jun. 2022, Art. no. 107109.
[2] X. Han, D. Jiang, X. Qu, Y. Bai, Y. Cao, R. Luo, and Z. Li, "A stretchable, self-healable triboelectric nanogenerator as electronic skin for energy harvesting and tactile sensing," *Materials*, vol. 14, no. 7, p. 1689, Mar. 2021.

[3] G. Zhu, Z.-H. Lin, Q. Jing, P. Bai, C. Pan, Y. Yang, Y. Zhou, and Z. L. Wang, "Toward large-scale energy harvesting by a nanoparticle-enhanced triboelectric nanogenerator," *Nano Lett.*, vol. 13, no. 2, pp. 847–853, Feb. 2013.

[4] F.-R. Fan, Z.-Q. Tian, and Z. Lin Wang, "Flexible triboelectric generator," *Nano Energy*, vol. 1, no. 2, pp. 328–334, Mar. 2012.

[5] L. Jingzhi and J. Yuan, "Preparation of triboelectric nanogenerators with CNT-containing and micro-structure PDMS composite films," *J. Mech. Eng.*, vol. 57, no. 15, p. 177, 2021.

[6] A. Yar, "High performance of multi-layered triboelectric nanogenerators for mechanical energy harvesting," *Energy*, vol. 222, May 2021, Art. no. 119949.

[7] J. Chen, G. Zhu, W. Yang, Q. Jing, P. Bai, Y. Yang, T.-C. Hou, and Z. L. Wang, "Harmonic-resonator-based triboelectric nanogenerator as a sustainable power source and a self-powered active vibration sensor," *Adv. Mater.*, vol. 25, no. 42, pp. 6094–6099, Nov. 2013.

[8] S. Liu, X. Li, Y. Wang, Y. Yang, L. Meng, T. Cheng, and Z. L. Wang, "Magnetic switch structured triboelectric nanogenerator for continuous and regular harvesting of wind energy," *Nano Energy*, vol. 83, May 2021, Art. no. 105851.

[9] U. T. Jurado, S. H. Pu, and N. M. White, "A contact-separation mode triboelectric nanogenerator for ocean wave impact energy harvesting," in *Proc. IEEE SENSORS*, Glasgow, U.K., Oct. 2017, pp. 1–3.

[10] S. Yong, J. Wang, L. Yang, H. Wang, H. Luo, R. Liao, and Z. L. Wang, "Auto-switching self-powered system for efficient broadband wind energy harvesting based on dual-rotation shaft triboelectric nanogenerator," *Adv. Energy Mater.*, vol. 11, no. 26, Jul. 2021, Art. no. 2101194.

[11] A. Song, Y. Han, H. Hu, and J. Li, "A novel texture sensor for fabric texture measurement and classification," *IEEE Trans. Instrum. Meas.*, vol. 63, no. 7, pp. 1739–1747, Jul. 2014.

[12] S. Lee, H. Nozawa, D. Watanabe, and K. Inoue, "Force estimation via physical properties of air cushion for the control of a human-cooperative robot: Basic experiments," *Adv. Robot.*, vol. 29, no. 2, pp. 139–146, Jan. 2015.

[13] Q. Jing, G. Zhu, W. Wu, P. Bai, Y. Xie, R. P. S. Han, and Z. L. Wang, "Self-powered triboelectric velocity sensor for dual-mode sensing of rectified linear and rotary motions," *Nano Energy*, vol. 10, pp. 305–312, Nov. 2014.

[14] Y. Yang, G. Zhu, H. Zhang, J. Chen, X. Zhong, Z.-H. Lin, Y. Su, P. Bai, X. Wen, and Z. L. Wang, "Triboelectric nanogenerator for harvesting wind energy and as self-powered wind vector sensor system," *ACS Nano*, vol. 7, no. 10, pp. 9461–9468, Sep. 2013.

[15] Y. S. Zhou, G. Zhu, S. Niu, Y. Liu, P. Bai, Q. Jing, and Z. L. Wang, "Nanometer resolution self-powered static and dynamic motion sensor based on micro-grated triboelectrification," *Adv. Mater.*, vol. 26, no. 11, pp. 1719–1724, Mar. 2014.

[16] Z. Lin, G. Zhu, and Y. S. Zhou, "A self-powered triboelectric nanosensor for mercury ion detection," *Angew. Chem. Int. Ed.*, vol. 52, no. 19, pp. 5065–5069, May 2013.

[17] H. Zhang, Y. Yang, Y. Su, J. Chen, C. Hu, Z. Wu, Y. Liu, C. Ping Wong, Y. Bando, and Z. L. Wang, "Triboelectric nanogenerator as self-powered active sensors for detecting liquid/gaseous water/ethanol," *Nano Energy*, vol. 2, no. 5, pp. 693–701, Sep. 2013.

[18] X. Wen, Y. Su, Y. Yang, H. Zhang, and Z. L. Wang, "Applicability of triboelectric generator over a wide range of temperature," *Nano Energy*, vol. 4, pp. 150–156, Mar. 2014.

[19] Y. Su, G. Zhu, W. Yang, J. Yang, J. Chen, Q. Jing, Z. Wu, Y. Jiang, and Z. L. Wang, "Triboelectric sensor for self-powered tracking of object motion inside tubing," *ACS Nano*, vol. 8, no. 4, pp. 3843–3850, Apr. 2014.

[20] F. Yi, L. Lin, S. Niu, J. Yang, W. Wu, S. Wang, Q. Liao, Y. Zhang, and Z. L. Wang, "Self-powered trajectory, velocity, and acceleration tracking of a moving object/body using a triboelectric sensor," *Adv. Funct. Mater.*, vol. 24, no. 47, pp. 7488–7494, Dec. 2014.

[21] C. B. Han, C. Zhang, X. H. Li, L. Zhang, T. Zhou, W. Hu, and Z. L. Wang, "Self-powered velocity and trajectory tracking sensor array made of planar triboelectric nanogenerator pixels," *Nano Energy*, vol. 9, pp. 325–333, Oct. 2014.

[22] Z. L. Wang, "Triboelectric nanogenerators as new energy technology for self-powered systems and as active mechanical and chemical sensors," *ACS Nano*, vol. 7, no. 11, pp. 9533–9557, Nov. 2013.

[23] Y.-W. Cai, G.-G. Wang, Y.-C. Mei, D.-Q. Zhao, J.-J. Peng, N. Sun, H.-Y. Zhang, J.-C. Han, and Y. Yang, "Self-healable, super-stretchable and shape-adaptive triboelectric nanogenerator based on double cross-linked PDMS for electronic skins," *Nano Energy*, vol. 102, Nov. 2022, Art. no. 107683.

[24] Y. Wang, Q. Zhu, and Z. Zhu, "Review of triboelectric nanogenerators applied to the field of intelligent robotics," in *Proc. 5th World Conf. Mech. Eng. Intell. Manuf. (WCMEIM)*, Maanshan, China, Nov. 2022, pp. 736–739.

[25] L. Hines, K. Petersen, G. Z. Lum, and M. Sitti, "Soft actuators for small-scale robotics," *Adv. Mater.*, vol. 29, no. 13, Apr. 2017, Art. no. 1603483.

[26] S. Kim, C. Laschi, and B. Trimmer, "Soft robotics: A bioinspired evolution in robotics," *Trends Biotechnol.*, vol. 31, no. 5, pp. 287–294, May 2013.

[27] S. Bauer, S. Bauer-Gogonea, I. Graz, M. Kaltenbrunner, C. Keplinger, and R. Schwödiauer, "25th anniversary article: A soft future: From robots and sensor skin to energy harvesters," *Adv. Mater.*, vol. 26, no. 1, pp. 149–162, Jan. 2014, doi: 10.1002/ADMA.201303349.

[28] M. A. McEvoy and N. Correll, "Materials that couple sensing, actuation, computation, and communication," *Science*, vol. 347, no. 6228, Mar. 2015, Art. no. 1261689.

[29] Z. L. Wang, J. Chen, and L. Lin, "Progress in triboelectric nanogenerators as a new energy technology and self-powered sensors," *Energy Environ. Sci.*, vol. 8, no. 8, pp. 2250–2282, 2015.

[30] I. Kim, H. Jeon, D. Kim, J. You, and D. Kim, "All-in-one cellulose based triboelectric nanogenerator for electronic paper using simple filtration process," *Nano Energy*, vol. 53, pp. 975–981, Nov. 2018.

[31] L. Xie, X. Chen, Z. Wen, Y. Yang, J. Shi, C. Chen, M. Peng, Y. Liu, and X. Sun, "Spiral steel wire based fiber-shaped stretchable and tailorable triboelectric nanogenerator for wearable power source and active gesture sensor," *Nano-Micro Lett.*, vol. 11, no. 1, p. 39, Dec. 2019.

[32] X. Zhang, Z. Li, W. Du, Y. Zhao, W. Wang, L. Pang, L. Chen, A. Yu, and J. Zhai, "Self-powered triboelectric-mechanoluminescent electronic skin for detecting and differentiating multiple mechanical stimuli," *Nano Energy*, vol. 96, Jun. 2022, Art. no. 107115.

[33] H. L. Wang, S. Y. Kuang, H. Y. Li, Z. L. Wang, and G. Zhu, "Large-area integrated triboelectric sensor array for wireless static and dynamic pressure detection and mapping," *Small*, vol. 16, no. 2, Jan. 2020, Art. no. 1906352.

[34] L. Zheng, S. Dong, J. Nie, S. Li, Z. Ren, X. Ma, X. Chen, H. Li, and Z. L. Wang, "Dual-stimulus smart actuator and robot hand based on a vapor-responsive PDMS film and triboelectric nanogenerator," *ACS Appl. Mater. Interfaces*, vol. 11, no. 45, pp. 42504–42511, Nov. 2019.

[35] S. A. Shankaregowda, R. F. S. M. Ahmed, C. B. Nanjegowda, J. Wang, S. Guan, M. Puttaswamy, A. Amini, Y. Zhang, D. Kong, K. Sannathammegowda, F. Wang, and C. Cheng, "Single-electrode triboelectric nanogenerator based on economical graphite coated paper for harvesting waste environmental energy," *Nano Energy*, vol. 66, Dec. 2019, Art. no. 104141.

[36] Y.-C. Lai, J. Deng, S. L. Zhang, S. Niu, H. Guo, and Z. L. Wang, "Single-thread-based wearable and highly stretchable triboelectric nanogenerators and their applications in cloth-based self-powered human-interactive and biomedical sensing," *Adv. Funct. Mater.*, vol. 27, no. 1, Jan. 2017, Art. no. 1604462.

[37] S. Zhang, B. Zhang, D. Zhao, Q. Gao, Z. L. Wang, and T. Cheng, "Nondestructive dimension sorting by soft robotic grippers integrated with triboelectric sensor," *ACS Nano*, vol. 16, no. 2, pp. 3008–3016, Feb. 2022.

[38] H. Park, S. Oh, D. Kim, M. Kim, C. Lee, H. Joo, I. Woo, J. W. Bae, and J. Lee, "Plasticized PVC-Gel single layer-based stretchable triboelectric nanogenerator for harvesting mechanical energy and tactile sensing," *Adv. Sci.*, vol. 9, no. 22, Aug. 2022, Art. no. 2201070.

[39] L. Jinchi, Y. Miao, and W. Xia, "Application of triboelectric nanogeneratorsin fabric-based intelligent wearable devices," *Adv. Textile Technol.*, vol. 28, no. 4, pp. 53–63, 2020.

[40] Z. Xu, D. Zhang, H. Cai, Y. Yang, H. Zhang, and C. Du, "Performance enhancement of triboelectric nanogenerators using contact-separation mode in conjunction with the sliding mode and multifunctional application for motion monitoring," *Nano Energy*, vol. 102, Nov. 2022, Art. no. 107719.

[41] Q. Yu, P. Jun-Le, Y. De-Chao, L. Bing, and W. Xiao-Na, "Generation characteristic analysis of spherical triboelectric nanogenerator based on COMOSL multiphysics," *Phys. Experimentation*, vol. 37, no. 9, pp. 1–11, 2017.
[42] J. K. Mainra, A. Kaur, G. Sapra, and P. Gaur, "Simulation and modelling of triboelectric nanogenerator for self-powered electronic devices," *IOP Conf. Ser., Mater. Sci. Eng.*, vol. 1225, no. 1, Feb. 2022, Art. no. 012012.
[43] A. A. Mathew and S. Vivekanandan, "Design and simulation of single-electrode mode triboelectric nanogenerator-based pulse sensor for healthcare applications using COMSOL multiphysics," *Energy Technol.*, vol. 10, no. 5, May 2022, Art. no. 2101130.
[44] P. Yin, K. C. Aw, X. Jiang, C. Xin, H. Guo, L. Tang, Y. Peng, and Z. Li, "Fish gills inspired parallel-cell triboelectric nanogenerator," *Nano Energy*, vol. 95, May 2022, Art. no. 106976.
[45] M. A. Adly, M. H. Arafa, and H. A. Hegazi, "Modeling and optimization of an inertial triboelectric motion sensor," *Nano Energy*, vol. 85, Jul. 2021, Art. no. 105952.
[46] Z. Chen, K. Dai, J. Chen, J. Zhuo, D. Zhao, R. Ma, X. Zhang, X. Li, X. Wang, G. Yang, and F. Yi, "Influence of the reference electrode on the performance of single–electrode triboelectric nanogenerators and the optimization strategies," *Adv. Sci.*, vol. 10, no. 17, Jun. 2023, Art. no. 2206950.
[47] J. Roopa, H. Swathi, K. S. Geetha, and B. S. Satyanaryana, "Modeling and simulation of triboelectric nanogenerator for energy harvesting using COMSOL Multiphysics® and optimization on thickness of flexible polymer," *Mater. Today, Proc.*, vol. 48, pp. 702–705, 2022.
[48] B. Cheng, Q. Xu, Y. Ding, S. Bai, X. Jia, Y. Yu, J. Wen, and Y. Qin, "High performance temperature difference triboelectric nanogenerator," *Nature Commun.*, vol. 12, no. 1, p. 4782, Aug. 2021.
[49] T. Bhatta, S. Sharma, K. Shrestha, Y. Shin, S. Seonu, S. Lee, D. Kim, M. Sharifuzzaman, S. S. Rana, and J. Y. Park, "Siloxene/PVDF composite nanofibrous membrane for high-performance triboelectric nanogenerator and self-powered static and dynamic pressure sensing applications," *Adv. Funct. Mater.*, vol. 32, no. 25, Jun. 2022, Art. no. 2202145.
[50] L. Na, M. Cheng-Xu, C. Hui, W. Jian-Wei, and Y. Xi-Ya, "Simulation study of a coupled system based on raft wave energy conversion and triboelectric nanogenerator energy output," *Adv. New Renew. Energy*, vol. 10, no. 3, pp. 265–270, 2022.
[51] Y.-S. Wu, L. Qi, C. Jie, L. Kai, C. Guang-Gui, Z. Zhong-Qiang, D. Jian-Ning, and J. Shi-Yu, "Design and output performance of vibration energy harvesting triboelectric nanogenerator," *Acta Phys. Sinca*, vol. 68, no. 19, 2019, Art. no. 190201.
[52] J. Chun, J. W. Kim, W.-S. Jung, C.-Y. Kang, S.-W. Kim, Z. L. Wang, and J. M. Baik, "Mesoporous pores impregnated with Au nanoparticles as effective dielectrics for enhancing triboelectric nanogenerator performance in harsh environments," *Energy Environ. Sci.*, vol. 8, no. 10, pp. 3006–3012, 2015.
[53] J. P. Lee, B. U. Ye, K. N. Kim, J. W. Lee, W. J. Choi, and J. M. Baik, "3D printed noise-cancelling triboelectric nanogenerator," *Nano Energy*, vol. 38, pp. 377–384, Aug. 2017.
[54] P. Bai, G. Zhu, Z.-H. Lin, Q. Jing, J. Chen, G. Zhang, J. Ma, and Z. L. Wang, "Integrated multilayered triboelectric nanogenerator for harvesting biomechanical energy from human motions," *ACS Nano*, vol. 7, no. 4, pp. 3713–3719, Apr. 2013.
[55] Y. Su, X. Wen, G. Zhu, J. Yang, J. Chen, P. Bai, Z. Wu, Y. Jiang, and Z. L. Wang, "Hybrid triboelectric nanogenerator for harvesting water wave energy and as a self-powered distress signal emitter," *Nano Energy*, vol. 9, pp. 186–195, Oct. 2014.
[56] X. Pu, M. Liu, L. Li, C. Zhang, Y. Pang, C. Jiang, L. Shao, W. Hu, and Z. L. Wang, "Efficient charging of Li-ion batteries with pulsed output current of triboelectric nanogenerators," *Adv. Sci.*, vol. 3, no. 1, Jan. 2016, Art. no. 1500255.
[57] P. Bai, G. Zhu, Q. Jing, J. Yang, J. Chen, Y. Su, J. Ma, G. Zhang, and Z. L. Wang, "Membrane-based self-powered triboelectric sensors for pressure change detection and its uses in security surveillance and healthcare monitoring," *Adv. Funct. Mater.*, vol. 24, no. 37, pp. 5807–5813, Oct. 2014.
[58] Y. Xie, S. Wang, S. Niu, L. Lin, Q. Jing, J. Yang, Z. Wu, and Z. L. Wang, "Grating-structured freestanding triboelectric-layer nanogenerator for harvesting mechanical energy at 85% total conversion efficiency," *Adv. Mater.*, vol. 26, no. 38, pp. 6599–6607, Oct. 2014.
[59] L. Lin, Y. Xie, S. Niu, S. Wang, P.-K. Yang, and Z. L. Wang, "Robust triboelectric nanogenerator based on rolling electrification and electrostatic induction at an instantaneous energy conversion efficiency of ~55%," *ACS Nano*, vol. 9, no. 1, pp. 922–930, Jan. 2015.
[60] L. Lin, S. Wang, Y. Xie, Q. Jing, S. Niu, Y. Hu, and Z. L. Wang, "Segmentally structured disk triboelectric nanogenerator for harvesting rotational mechanical energy," *Nano Lett.*, vol. 13, no. 6, pp. 2916–2923, Jun. 2013.
[61] Z. Zhao, X. Pu, C. Du, L. Li, C. Jiang, W. Hu, and Z. L. Wang, "Freestanding flag-type triboelectric nanogenerator for harvesting high-altitude wind energy from arbitrary directions," *ACS Nano*, vol. 10, no. 2, pp. 1780–1787, Feb. 2016.
[62] A. Yu, Y. Zhu, W. Wang, and J. Zhai, "Progress in triboelectric materials: Toward high performance and widespread applications," *Adv. Funct. Mater.*, vol. 29, no. 41, Oct. 2019, Art. no. 1900098.
[63] F.-R. Fan, L. Lin, G. Zhu, W. Wu, R. Zhang, and Z. L. Wang, "Transparent triboelectric nanogenerators and self-powered pressure sensors based on micropatterned plastic films," *Nano Lett.*, vol. 12, no. 6, pp. 3109–3114, Jun. 2012.
[64] L. Zhao, Q. Zheng, H. Ouyang, H. Li, L. Yan, B. Shi, and Z. Li, "A size-unlimited surface microstructure modification method for achieving high performance triboelectric nanogenerator," *Nano Energy*, vol. 28, pp. 172–178, Oct. 2016.
[65] M. Shi, J. Zhang, H. Chen, M. Han, S. A. Shankaregowda, Z. Su, B. Meng, X. Cheng, and H. Zhang, "Self-powered analogue smart skin," *ACS Nano*, vol. 10, no. 4, pp. 4083–4091, Apr. 2016.
[66] W. He, M. Sohn, R. Ma, and D. J. Kang, "Flexible single-electrode triboelectric nanogenerators with MXene/PDMS composite film for biomechanical motion sensors," *Nano Energy*, vol. 78, Dec. 2020, Art. no. 105383.
[67] B. Dudem, R. D. I. G. Dharmasena, S. A. Graham, J. W. Leem, H. Patnam, A. R. Mule, S. R. P. Silva, and J. S. Yu, "Exploring the theoretical and experimental optimization of high-performance triboelectric nanogenerators using microarchitectured silk cocoon films," *Nano Energy*, vol. 74, Aug. 2020, Art. no. 104882.
[68] G. Yao, "Bioinspired triboelectric nanogenerators as self-powered electronic skin for robotic tactile sensing," *Adv. Funct. Mater.*, vol. 30, no. 6, p. 1907312, 2020.
[69] W. Sun, B. Li, F. Zhang, C. Fang, Y. Lu, X. Gao, C. Cao, G. Chen, C. Zhang, and Z. L. Wang, "TENG-bot: Triboelectric nanogenerator powered soft robot made of uni-directional dielectric elastomer," *Nano Energy*, vol. 85, Jul. 2021, Art. no. 106012.
[70] H. Fang, W. Wu, J. Song, and Z. L. Wang, "Controlled growth of aligned polymer nanowires," *J. Phys. Chem. C*, vol. 113, no. 38, pp. 16571–16574, Sep. 2009.
[71] X.-S. Zhang, M.-D. Han, R.-X. Wang, F.-Y. Zhu, Z.-H. Li, W. Wang, and H.-X. Zhang, "Frequency-multiplication high-output triboelectric nanogenerator for sustainably powering biomedical microsystems," *Nano Lett.*, vol. 13, no. 3, pp. 1168–1172, Mar. 2013.
[72] W. Jing, M. Wen, C. Huisheng, and L. Liang, "Study on properties of composite triboelectric-materials films," *Inf. Recording Mater.*, vol. 20, no. 10, pp. 7–10, 2019.
[73] Y. Liu, J. Mo, Q. Fu, Y. Lu, N. Zhang, S. Wang, and S. Nie, "Enhancement of triboelectric charge density by chemical functionalization," *Adv. Funct. Mater.*, vol. 30, no. 50, Dec. 2020, Art. no. 2004714.
[74] D. Jang, Y. Kim, T. Y. Kim, K. Koh, U. Jeong, and J. Cho, "Force-assembled triboelectric nanogenerator with high-humidity-resistant electricity generation using hierarchical surface morphology," *Nano Energy*, vol. 20, pp. 283–293, Feb. 2016.
[75] D. Chen, C. Ni, L. Xie, Y. Li, S. Deng, Q. Zhao, and T. Xie, "Homeostatic growth of dynamic covalent polymer network toward ultrafast direct soft lithography," *Sci. Adv.*, vol. 7, no. 43, Oct. 2021, Art. no. eabi7360.
[76] C. K. Jeong, K. M. Baek, S. Niu, T. W. Nam, Y. H. Hur, D. Y. Park, G.-T. Hwang, M. Byun, Z. L. Wang, Y. S. Jung, and K. J. Lee, "Topographically-designed triboelectric nanogenerator via block copolymer self-assembly," *Nano Lett.*, vol. 14, no. 12, pp. 7031–7038, Dec. 2014.
[77] G. Zhu, C. Pan, W. Guo, C.-Y. Chen, Y. Zhou, R. Yu, and Z. L. Wang, "Triboelectric-generator-driven pulse electrodeposition for micropatterning," *Nano Lett.*, vol. 12, no. 9, pp. 4960–4965, Sep. 2012.
[78] Y. Yang, H. Zhang, Z.-H. Lin, Y. S. Zhou, Q. Jing, Y. Su, J. Yang, J. Chen, C. Hu, and Z. L. Wang, "Human skin based triboelectric nanogenerators for harvesting biomechanical energy and as self-powered active tactile sensor system," *ACS Nano*, vol. 7, no. 10, pp. 9213–9222, Oct. 2013.

[79] Z. Man, S. Cheng, X. Liangping, D. Suihu, Z. Mengting, and D. Chunlei, "Flexible single-electrode triboelectric nanogenerator based on polydimethylsiloxane microstructures," *Micronanoelectronic Technol.*, vol. 59, no. 1, pp. 44–49, 2022.

[80] G. Du, J. Wang, Y. Liu, J. Yuan, T. Liu, C. Cai, B. Luo, S. Zhu, Z. Wei, S. Wang, and S. Nie, "Fabrication of advanced cellulosic triboelectric materials via dielectric modulation," *Adv. Sci.*, vol. 10, no. 15, Mar. 2023, Art. no. 2206243.

[81] M. Khalifa and S. Anandhan, "PVDF nanofibers with embedded polyaniline–graphitic carbon nitride nanosheet composites for piezoelectric energy conversion," *ACS Appl. Nano Mater.*, vol. 2, no. 11, pp. 7328–7339, Nov. 2019.

[82] H. Ouyang, J. Tian, G. Sun, Y. Zou, Z. Liu, H. Li, L. Zhao, B. Shi, Y. Fan, Y. Fan, Z. L. Wang, and Z. Li, "Self-powered pulse sensor for antidiastole of cardiovascular disease," *Adv. Mater.*, vol. 29, no. 40, Oct. 2017, Art. no. 1703456.

[83] X.-S. Zhang, M.-D. Han, R.-X. Wang, B. Meng, F.-Y. Zhu, X.-M. Sun, W. Hu, W. Wang, Z.-H. Li, and H.-X. Zhang, "High-performance triboelectric nanogenerator with enhanced energy density based on single-step fluorocarbon plasma treatment," *Nano Energy*, vol. 4, pp. 123–131, Mar. 2014.

[84] B. K. Yun, J. W. Kim, H. S. Kim, K. W. Jung, Y. Yi, M.-S. Jeong, J.-H. Ko, and J. H. Jung, "Base-treated polydimethylsiloxane surfaces as enhanced triboelectric nanogenerators," *Nano Energy*, vol. 15, pp. 523–529, Jul. 2015.

[85] H. Y. Li, L. Su, S. Y. Kuang, C. F. Pan, G. Zhu, and Z. L. Wang, "Significant enhancement of triboelectric charge density by fluorinated surface modification in nanoscale for converting mechanical energy," *Adv. Funct. Mater.*, vol. 25, no. 35, pp. 5691–5697, Sep. 2015.

[86] Z. L. Wang, "On the first principle theory of nanogenerators from Maxwell's equations," *Nano Energy*, vol. 68, Feb. 2020, Art. no. 104272.

[87] H. Chen, Y. Song, X. Cheng, and H. Zhang, "Self-powered electronic skin based on the triboelectric generator," *Nano Energy*, vol. 56, pp. 252–268, Feb. 2019.

[88] J. Henniker, "Triboelectricity in polymers," *Nature*, vol. 196, no. 4853, pp. 474–473, Nov. 1962.

[89] D. K. Davies, "Charge generation on dielectric surfaces," *J. Phys. D, Appl. Phys.*, vol. 2, no. 11, pp. 1533–1537, Nov. 1969.

[90] M. A. Narayanan, T. M. Haddad, A. Smer, M. Ayan, and A. Mooss, "Cocaine toxicity presenting as acute reversible pulmonary hypertension and right heart failure," *J. Amer. College Cardiol.*, vol. 65, no. 10, p. A645, Mar. 2015.

[91] Q. Zheng, B. Shi, Z. Li, and Z. L. Wang, "Recent progress on piezoelectric and triboelectric energy harvesters in biomedical systems," *Adv. Sci.*, vol. 4, no. 7, Jul. 2017, Art. no. 1700029.

[92] T. Jing, B. Xu, X. Guan, Y. Yang, M. Wu, and C. Jiang, "Liquid-filling polydimethylsiloxane composites with enhanced triboelectric performance for flexible nanogenerators," *Macromolecular Mater. Eng.*, vol. 305, no. 9, Sep. 2020, Art. no. 2000275.

[93] D. W. Kim, J. H. Lee, J. K. Kim, and U. Jeong, "Material aspects of triboelectric energy generation and sensors," *NPG Asia Mater.*, vol. 12, no. 1, p. 6, Dec. 2020.

[94] M. Matsunaga, J. Hirotani, S. Kishimoto, and Y. Ohno, "High-output, transparent, stretchable triboelectric nanogenerator based on carbon nanotube thin film toward wearable energy harvesters," *Nano Energy*, vol. 67, Jan. 2020, Art. no. 104297.

[95] G.-Z. Li, G.-G. Wang, Y.-W. Cai, N. Sun, F. Li, H.-L. Zhou, H.-X. Zhao, X.-N. Zhang, J.-C. Han, and Y. Yang, "A high-performance transparent and flexible triboelectric nanogenerator based on hydrophobic composite films," *Nano Energy*, vol. 75, Sep. 2020, Art. no. 104918.

[96] Z. Ding, M. Zou, P. Yao, and L. Fan, "A triboelectric nanogenerator for mechanical energy harvesting and as self-powered pressure sensor," *Microelectronic Eng.*, vol. 257, Mar. 2022, Art. no. 111725.

[97] J. Wang, P. Cui, J. Zhang, Y. Ge, X. Liu, N. Xuan, G. Gu, G. Cheng, and Z. Du, "A stretchable self-powered triboelectric tactile sensor with EGaIn alloy electrode for ultra-low-pressure detection," *Nano Energy*, vol. 89, Nov. 2021, Art. no. 106320.

[98] Z. Wang, T. Bu, Y. Li, D. Wei, B. Tao, Z. Yin, C. Zhang, and H. Wu, "Multidimensional force sensors based on triboelectric nanogenerators for electronic skin," *ACS Appl. Mater. Interfaces*, vol. 13, no. 47, pp. 56320–56328, Dec. 2021.

[99] X. Qu, Z. Liu, P. Tan, C. Wang, Y. Liu, H. Feng, D. Luo, Z. Li, and Z. L. Wang, "Artificial tactile perception smart finger for material identification based on triboelectric sensing," *Sci. Adv.*, vol. 8, no. 31, Aug. 2022, Art. no. eabq2521.

[100] B. Chen, W. Tang, and Z. L. Wang, "Advanced 3D printing-based triboelectric nanogenerator for mechanical energy harvesting and self-powered sensing," *Mater. Today*, vol. 50, pp. 224–238, Nov. 2021.

[101] M. Kanik, M. G. Say, B. Daglar, A. F. Yavuz, M. H. Dolas, M. M. El-Ashry, and M. Bayindir, "A motion- and sound-activated, 3D-printed, chalcogenide-based triboelectric nanogenerator," *Adv. Mater.*, vol. 27, no. 14, pp. 2367–2376, Apr. 2015.

[102] X. Zhou, K. Parida, O. Halevi, and Y. Liu, "All 3D-printed stretchable piezoelectric nanogenerator with non-protruding kirigami structure," *Nano Energy*, vol. 72, Jun. 2020, Art. no. 104676.

[103] R. I. Haque, O. Chandran, S. Lani, and D. Briand, "Self-powered triboelectric touch sensor made of 3D printed materials," *Nano Energy*, vol. 52, pp. 54–62, Oct. 2018.

[104] H. Li, R. Li, X. Fang, H. Jiang, X. Ding, B. Tang, G. Zhou, R. Zhou, and Y. Tang, "3D printed flexible triboelectric nanogenerator with viscoelastic inks for mechanical energy harvesting," *Nano Energy*, vol. 58, pp. 447–454, Apr. 2019.

[105] S. Chen, T. Huang, H. Zuo, S. Qian, Y. Guo, L. Sun, D. Lei, Q. Wu, B. Zhu, C. He, X. Mo, E. Jeffries, H. Yu, and Z. You, "A single integrated 3D-printing process customizes elastic and sustainable triboelectric nanogenerators for wearable electronics," *Adv. Funct. Mater.*, vol. 28, no. 46, Nov. 2018, Art. no. 1805108.

[106] A. Ahmed, I. Hassan, I. M. Mosa, E. Elsanadidy, G. S. Phadke, M. F. El-Kady, J. F. Rusling, P. R. Selvaganapathy, and R. B. Kaner, "All printable snow-based triboelectric nanogenerator," *Nano Energy*, vol. 60, pp. 17–25, Jun. 2019.

[107] K. Chen, L. Zhang, X. Kuang, V. Li, M. Lei, G. Kang, Z. L. Wang, and H. J. Qi, "Dynamic photomask-assisted direct ink writing multimaterial for multilevel triboelectric nanogenerator," *Adv. Funct. Mater.*, vol. 29, no. 33, Aug. 2019, Art. no. 1903568.

[108] F. Arab Hassani, R. P. Mogan, G. G. L. Gammad, H. Wang, S.-C. Yen, N. V. Thakor, and C. Lee, "Toward self-control systems for neurogenic underactive bladder: A triboelectric nanogenerator sensor integrated with a bistable micro-actuator," *ACS Nano*, vol. 12, no. 4, pp. 3487–3501, Apr. 2018.

[109] B. Chen, Z. Guo, S. Zeng, Y. Tian, S. Miao, and B. Zheng, "Paste structure and rheological properties of lotus seed starch–glycerin monostearate complexes formed by high-pressure homogenization," *Food Res. Int.*, vol. 103, pp. 380–389, Jan. 2018.

[110] S. S. K. Mallineni, Y. Dong, H. Behlow, A. M. Rao, and R. Podila, "A wireless triboelectric nanogenerator," *Adv. Energy Mater.*, vol. 8, no. 10, Apr. 2018, Art. no. 1702736.

[111] S. He, Z. Yu, H. Zhou, and Z. Huang, "Polymer tubes as carrier boats of thermosetting and powder materials based on 3D printing for triboelectric nanogenerator with microstructure," *Nano Energy*, vol. 52, pp. 134–141, Oct. 2018.

[112] S. Gao, Y. Zhu, Y. Chen, M. Tian, Y. Yang, T. Jiang, and Z. L. Wang, "Self-power electroreduction of N_2into NH_3 by 3D printed triboelectric nanogenerators," *Mater. Today*, vol. 28, pp. 17–24, Sep. 2019.

[113] C. Wu, H. Tetik, J. Cheng, W. Ding, H. Guo, X. Tao, N. Zhou, Y. Zi, Z. Wu, H. Wu, D. Lin, and Z. L. Wang, "Electrohydrodynamic jet printing driven by a triboelectric nanogenerator," *Adv. Funct. Mater.*, vol. 29, no. 22, May 2019, Art. no. 1901102.

[114] D. Hong, Y.-M. Choi, Y. Jang, and J. Jeong, "A multilayer thin-film screen-printed triboelectric nanogenerator," *Int. J. Energy Res.*, vol. 42, no. 11, pp. 3688–3695, Sep. 2018.

[115] Y. Zou, P. Tan, B. Shi, H. Ouyang, D. Jiang, Z. Liu, H. Li, M. Yu, C. Wang, X. Qu, L. Zhao, Y. Fan, Z. L. Wang, and Z. Li, "A bionic stretchable nanogenerator for underwater sensing and energy harvesting," *Nature Commun.*, vol. 10, no. 1, p. 2695, Jun. 2019.

[116] A. Yu, X. Chen, R. Wang, J. Liu, J. Luo, L. Chen, Y. Zhang, W. Wu, C. Liu, H. Yuan, M. Peng, W. Hu, J. Zhai, and Z. L. Wang, "Triboelectric nanogenerator as a self-powered communication unit for processing and transmitting information," *ACS Nano*, vol. 10, no. 4, pp. 3944–3950, Apr. 2016.

[117] X. Pu, M. Liu, X. Chen, J. Sun, C. Du, Y. Zhang, J. Zhai, W. Hu, and Z. L. Wang, "Ultrastretchable, transparent triboelectric nanogenerator as electronic skin for biomechanical energy harvesting and tactile sensing," *Sci. Adv.*, vol. 3, no. 5, May 2017, Art. no. e1700015.

[118] Y. Lee, J. Kim, B. Jang, S. Kim, B. K. Sharma, J.-H. Kim, and J.-H. Ahn, "Graphene-based stretchable/wearable self-powered touch sensor," *Nano Energy*, vol. 62, pp. 259–267, Aug. 2019.
[119] H. Zhang, D.-Z. Zhang, D.-Y. Wang, Z.-Y. Xu, Y. Yang, and B. Zhang, "Flexible single-electrode triboelectric nanogenerator with MWCNT/PDMS composite film for environmental energy harvesting and human motion monitoring," *Rare Met.*, vol. 41, no. 9, pp. 3117–3128, Sep. 2022.
[120] T. Bu, T. Xiao, Z. Yang, G. Liu, X. Fu, J. Nie, T. Guo, Y. Pang, J. Zhao, F. Xi, C. Zhang, and Z. L. Wang, "Stretchable triboelectric-photonic smart skin for tactile and gesture sensing," *Adv. Mater.*, vol. 30, no. 16, Apr. 2018, Art. no. 1800066.
[121] K. Xia, Z. Zhu, H. Zhang, and Z. Xu, "A triboelectric nanogenerator as self-powered temperature sensor based on PVDF and PTFE," *Appl. Phys. A, Solids Surf.*, vol. 124, no. 8, p. 520, Aug. 2018.
[122] J. Xiong, H. Luo, D. Gao, X. Zhou, P. Cui, G. Thangavel, K. Parida, and P. S. Lee, "Self-restoring, waterproof, tunable microstructural shape memory triboelectric nanogenerator for self-powered water temperature sensor," *Nano Energy*, vol. 61, pp. 584–593, Jul. 2019.
[123] K. Fan, D. Wei, Y. Zhang, P. Wang, K. Tao, and R. Yang, "A whirligig-inspired intermittent-contact triboelectric nanogenerator for efficient low-frequency vibration energy harvesting," *Nano Energy*, vol. 90, Dec. 2021, Art. no. 106576.
[124] W. Nie, "A sliding hybrid triboelectric-electromagnetic nanogenerator with staggered electrodes for human motion posture," *Energy Rep.*, vol. 8, pp. 617–625, Nov. 2022.
[125] L. Jin, J. Tao, R. Bao, L. Sun, and C. Pan, "Self-powered real-time movement monitoring sensor using triboelectric nanogenerator technology," *Sci. Rep.*, vol. 7, no. 1, p. 10521, Sep. 2017.
[126] L. Li, T. Wang, T. Jin, P. Ma, Y. Jiang, G. Yuan, and Y. Tian, "Research on shape perception of the soft gripper based on triboelectric nanogenerator," in *Proc. IEEE Int. Conf. Robot. Biomimetics (ROBIO)*, Dec. 2019, pp. 211–216.
[127] T. Jin, Z. Sun, L. Li, Q. Zhang, M. Zhu, Z. Zhang, G. Yuan, T. Chen, Y. Tian, X. Hou, and C. Lee, "Triboelectric nanogenerator sensors for soft robotics aiming at digital twin applications," *Nature Commun.*, vol. 11, no. 1, p. 5381, Oct. 2020.
[128] C. Li, Z. Wang, S. Shu, and W. Tang, "A self-powered vector angle/displacement sensor based on triboelectric nanogenerator," *Micromachines*, vol. 12, no. 3, p. 231, Feb. 2021.
[129] Q. Hua, J. Sun, H. Liu, R. Bao, R. Yu, J. Zhai, C. Pan, and Z. L. Wang, "Skin-inspired highly stretchable and conformable matrix networks for multifunctional sensing," *Nature Commun.*, vol. 9, no. 1, p. 244, Jan. 2018.
[130] C. Zhang, S. Liu, X. Huang, W. Guo, Y. Li, and H. Wu, "A stretchable dual-mode sensor array for multifunctional robotic electronic skin," *Nano Energy*, vol. 62, pp. 164–170, Aug. 2019.
[131] S. Wagner and S. Bauer, "Materials for stretchable electronics," *MRS Bull.*, vol. 37, no. 3, pp. 207–213, Mar. 2012.
[132] C. Wang, C. Wang, Z. Huang, and S. Xu, "Materials and structures toward soft electronics," *Adv. Mater.*, vol. 30, no. 50, Dec. 2018, Art. no. 1801368.
[133] F. R. Fan, W. Tang, and Z. L. Wang, "Flexible nanogenerators for energy harvesting and self-powered electronics," *Adv. Mater.*, vol. 28, no. 22, pp. 4283–4305, Jun. 2016.
[134] R. Hinchet, H.-J. Yoon, H. Ryu, M.-K. Kim, E.-K. Choi, D.-S. Kim, and S.-W. Kim, "Transcutaneous ultrasound energy harvesting using capacitive triboelectric technology," *Science*, vol. 365, no. 6452, pp. 491–494, Aug. 2019.
[135] S. Wang, Y. Xie, S. Niu, L. Lin, C. Liu, Y. S. Zhou, and Z. L. Wang, "Maximum surface charge density for triboelectric nanogenerators achieved by ionized-air injection: Methodology and theoretical understanding," *Adv. Mater.*, vol. 26, no. 39, pp. 6720–6728, Oct. 2014.
[136] L. Xu, H. Wu, G. Yao, L. Chen, X. Yang, B. Chen, X. Huang, W. Zhong, X. Chen, Z. Yin, and Z. L. Wang, "Giant voltage enhancement via triboelectric charge supplement channel for self-powered electroadhesion," *ACS Nano*, vol. 12, no. 10, pp. 10262–10271, Oct. 2018.
[137] W. Seung, M. K. Gupta, K. Y. Lee, K.-S. Shin, J.-H. Lee, T. Y. Kim, S. Kim, J. Lin, J. H. Kim, and S.-W. Kim, "Nanopatterned textile-based wearable triboelectric nanogenerator," *ACS Nano*, vol. 9, no. 4, pp. 3501–3509, Apr. 2015.
[138] Z. Yuan, G. Shen, C. Pan, and Z. L. Wang, "Flexible sliding sensor for simultaneous monitoring deformation and displacement on a robotic hand/arm," *Nano Energy*, vol. 73, Jul. 2020, Art. no. 104764.
[139] J. Zhu, Y. Zhu, and X. Wang, "A hybrid piezoelectric and triboelectric nanogenerator with PVDF nanoparticles and leaf-shaped microstructure PTFE film for scavenging mechanical energy," *Adv. Mater. Interfaces*, vol. 5, no. 2, Jan. 2018, Art. no. 1700750.
[140] L. Cheng, M. Yuan, L. Gu, Z. Wang, Y. Qin, T. Jing, and Z. L. Wang, "Wireless, power-free and implantable nanosystem for resistance-based biodetection," *Nano Energy*, vol. 15, pp. 598–606, Jul. 2015.
[141] A. Yu, L. Chen, X. Chen, A. Zhang, F. Fan, Y. Zhan, and Z. L. Wang, "Triboelectric sensor as self-powered signal reader for scanning probe surface topography imaging," *Nanotechnology*, vol. 26, no. 16, Apr. 2015, Art. no. 165501.
[142] M. Ha, J. Park, Y. Lee, and H. Ko, "Triboelectric generators and sensors for self-powered wearable electronics," *ACS Nano*, vol. 9, no. 4, pp. 3421–3427, Apr. 2015.
[143] H. S. Lee, J. Chung, G.-T. Hwang, C. K. Jeong, Y. Jung, J.-H. Kwak, H. Kang, M. Byun, W. D. Kim, S. Hur, S.-H. Oh, and K. J. Lee, "Flexible inorganic piezoelectric acoustic nanosensors for biomimetic artificial hair cells," *Adv. Funct. Mater.*, vol. 24, no. 44, pp. 6914–6921, Nov. 2014.
[144] S. H. Lee, C. K. Jeong, G.-T. Hwang, and K. J. Lee, "Self-powered flexible inorganic electronic system," *Nano Energy*, vol. 14, pp. 111–125, May 2015.
[145] J. Yang, J. Chen, Y. Su, Q. Jing, Z. Li, F. Yi, X. Wen, Z. Wang, and Z. L. Wang, "Eardrum-inspired active sensors for self-powered cardiovascular system characterization and throat-attached anti-interference voice recognition," *Adv. Mater.*, vol. 27, no. 8, pp. 1316–1326, Feb. 2015.
[146] Y. Hu, J. Yang, Q. Jing, S. Niu, W. Wu, and Z. L. Wang, "Triboelectric nanogenerator built on suspended 3D spiral structure as vibration and positioning sensor and wave energy harvester," *ACS Nano*, vol. 7, no. 11, pp. 10424–10432, Nov. 2013.
[147] L. Dhakar, F. E. H. Tay, and C. Lee, "Investigation of contact electrification based broadband energy harvesting mechanism using elastic PDMS microstructures," *J. Micromech. Microeng.*, vol. 24, no. 10, Oct. 2014, Art. no. 104002.
[148] H. Guo, J. Zhao, Q. Dong, L. Wang, X. Ren, S. Liu, C. Zhang, and G. Dong, "A self-powered and high-voltage-isolated organic optical communication system based on triboelectric nanogenerators and solar cells," *Nano Energy*, vol. 56, pp. 391–399, Feb. 2019.
[149] L. Hai-Sheng, F. Shuai, and W. Xuan, "Principle of triboelectric nanogenerator and its application in bionic and soft robot," *J. Funct. Mater. Devices*, vol. 27, no. 4, pp. 340–348, 2021.

ZHONGYANG XU was born in Heilongjiang, China, in 1999. He received the bachelor's degree from Heilongjiang University, in 2021, where he is currently pursuing the master's degree. His research focuses on flexible sensors.

JIABIN ZHANG was born in Heilongjiang, China, in 1997. He received the bachelor's degree from Qiqihar University, in 2019. He is currently pursuing the master's degree with Heilongjiang University. His research focuses on the IoT robotics and image recognition.

JUNHAN HUANG was born in Chongqing, China, in 1998. He received the bachelor's degree from Chongqing Jiaotong University in 2020. He is currently pursuing the master's degree with Heilongjiang University. His research focuses on mechanical design and manufacturing.

ZHONGXIAN WANG was born in Heilongjiang, China, in 1982. He received the B.S. degree in electrical engineering from the Harbin University of Science and Technology, Harbin, China, in 2004, and the M.S. degree in control and instrument engineering from Wonkwang University, Iksan, South Korea, in 2007.

He is currently a Senior Engineer with the School of Mechanical and Electrical Engineering, Heilongjiang University, Harbin. His research interests include high-frequency power conversion techniques and wireless power transmission techniques and their applications.

YONG SHI was born in Hubei, China, in 1973. He received the B.S. and Ph.D. degrees in mechanical engineering from the Harbin Institute of Technology, Harbin, China, in 1995 and 2004, respectively, and the M.Sc. degree in mechatronics engineering from Auckland University, in 2022. During his master's study, his work focused on developing and applying soft and stretchable sensors.

He is a Professor with the School of Mechanical and Electrical Engineering, Heilongjiang University, Harbin. His research interests include mechanical design, sensors, and actuators in various applications.